



Massachusetts Institute of Technology



International Center for
Quantum-field Measurement Systems for
Studies of the Universe and Particles
WPI research center at KEK

Preliminary

Light Dark Matter Search with NV Centers: Electron Spin, Nuclear Spin, Comagnetometry

In collaboration with

M. Hazumi, E. D. Herbschleb, N. Mizuuchi, K. Nakayama, Y. Matsuzaki
J. High Energ. Phys. 2025, 83 (2025) [arXiv: 2302.12756]
Phys. Rev. D 111 (2025) 075028 [arXiv: 2407.07141]
Preliminary works

1 minute summary

① Introduction to dark matter

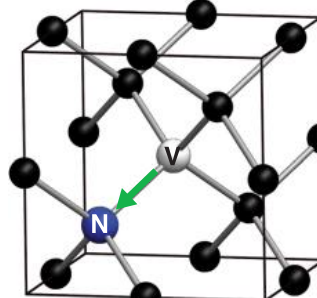
①

- NV center is a lattice defect in diamond
- Used as quantum sensing device
 - Measurement of electron spin
 - Control on electron/nitrogen spins

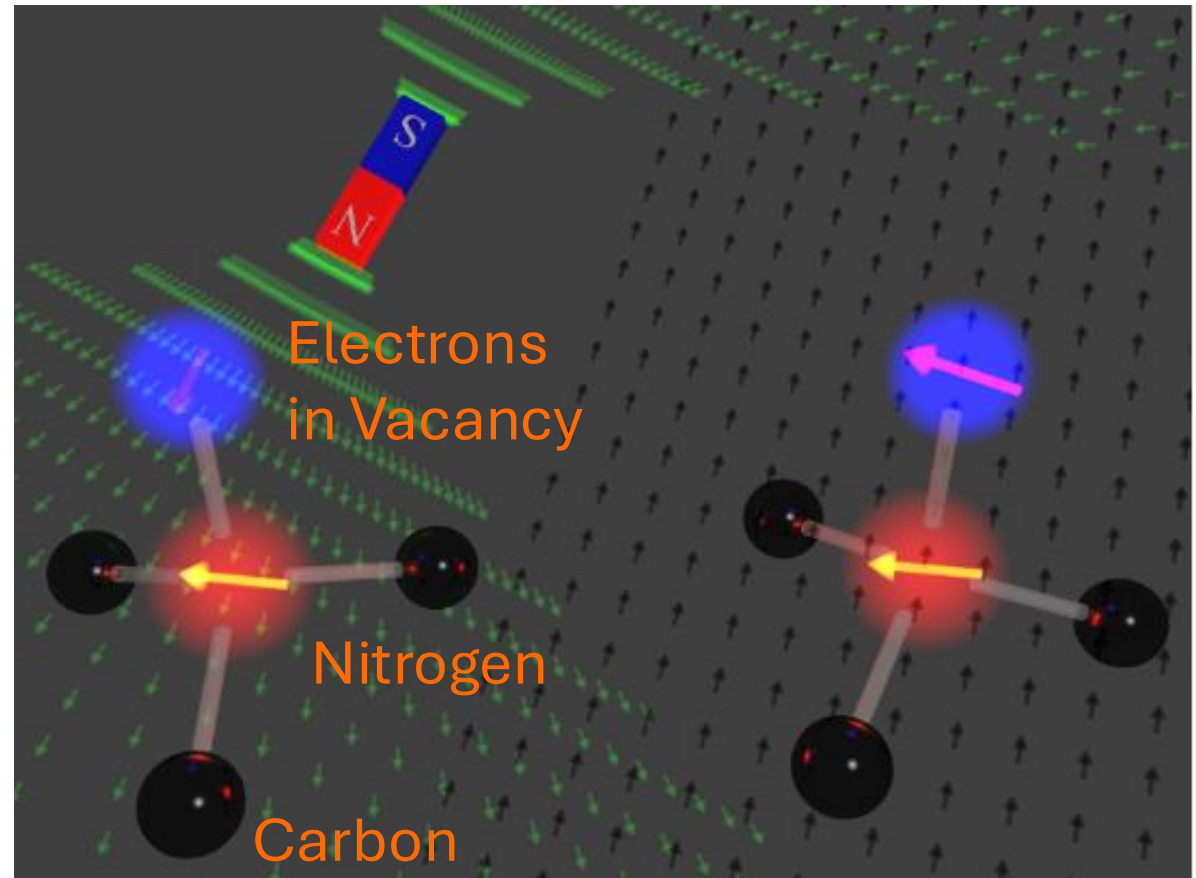
②

- With electron spins
 - (Dark matter-induced) \vec{B} -field
- ③
- With nitrogen spins
 - Dark matter-nuclear spin interaction
 - Comagnetometry
- ④
- Hybrid dynamical decoupling

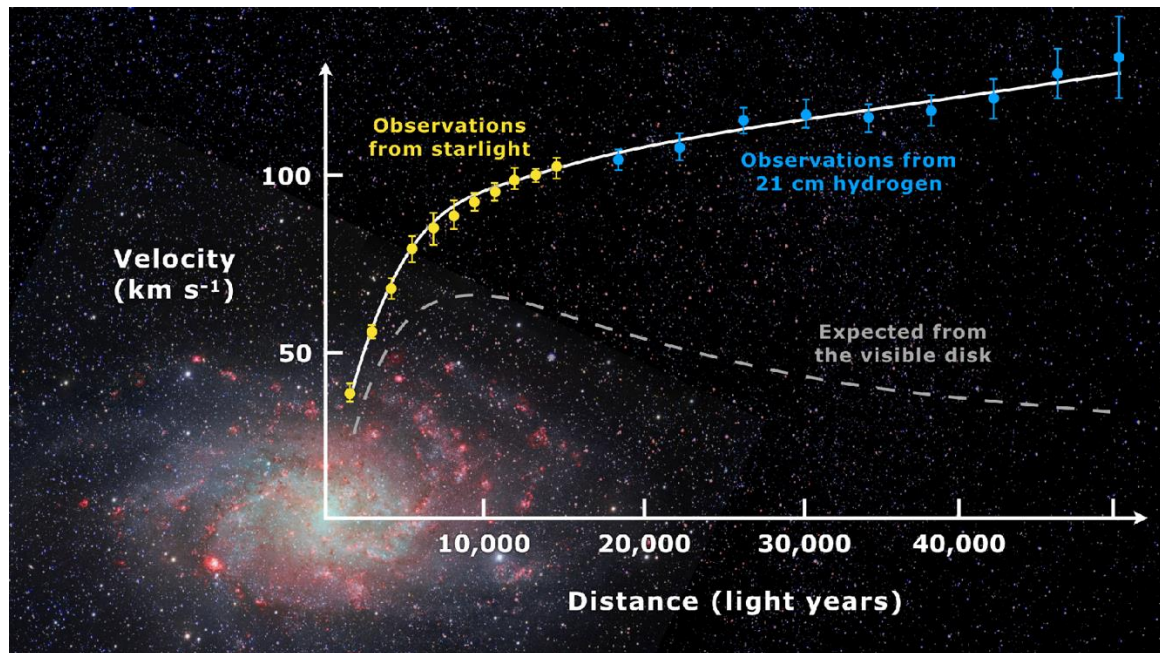
(a)



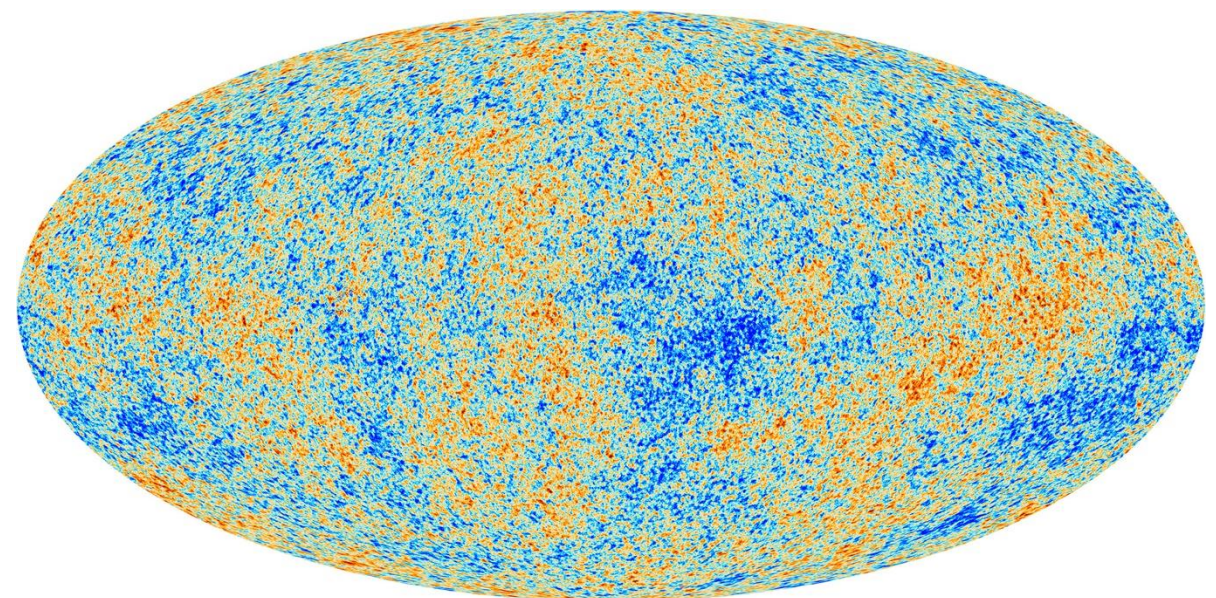
L. M. Pham '13



① Dark Matter as a hint of new physics



E. Corbelli, P. Salucci (2000)



Planck Collaboration

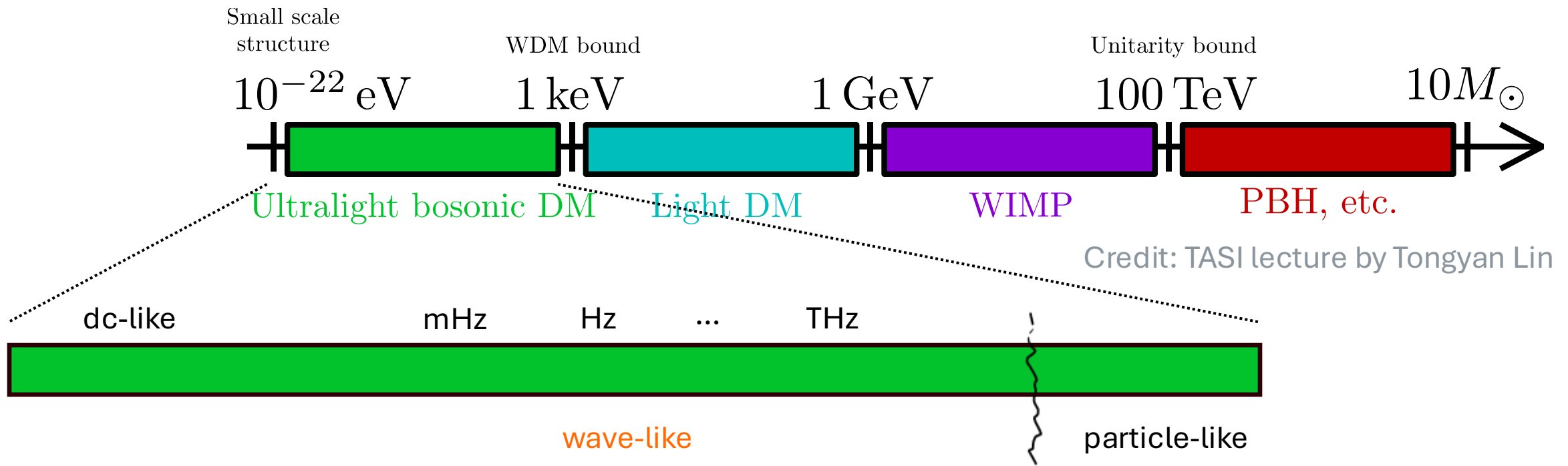
Knowns

- DM existence, abundance
- Has gravitational interaction

Unknowns

- Mass
- Non-gravitational interactions

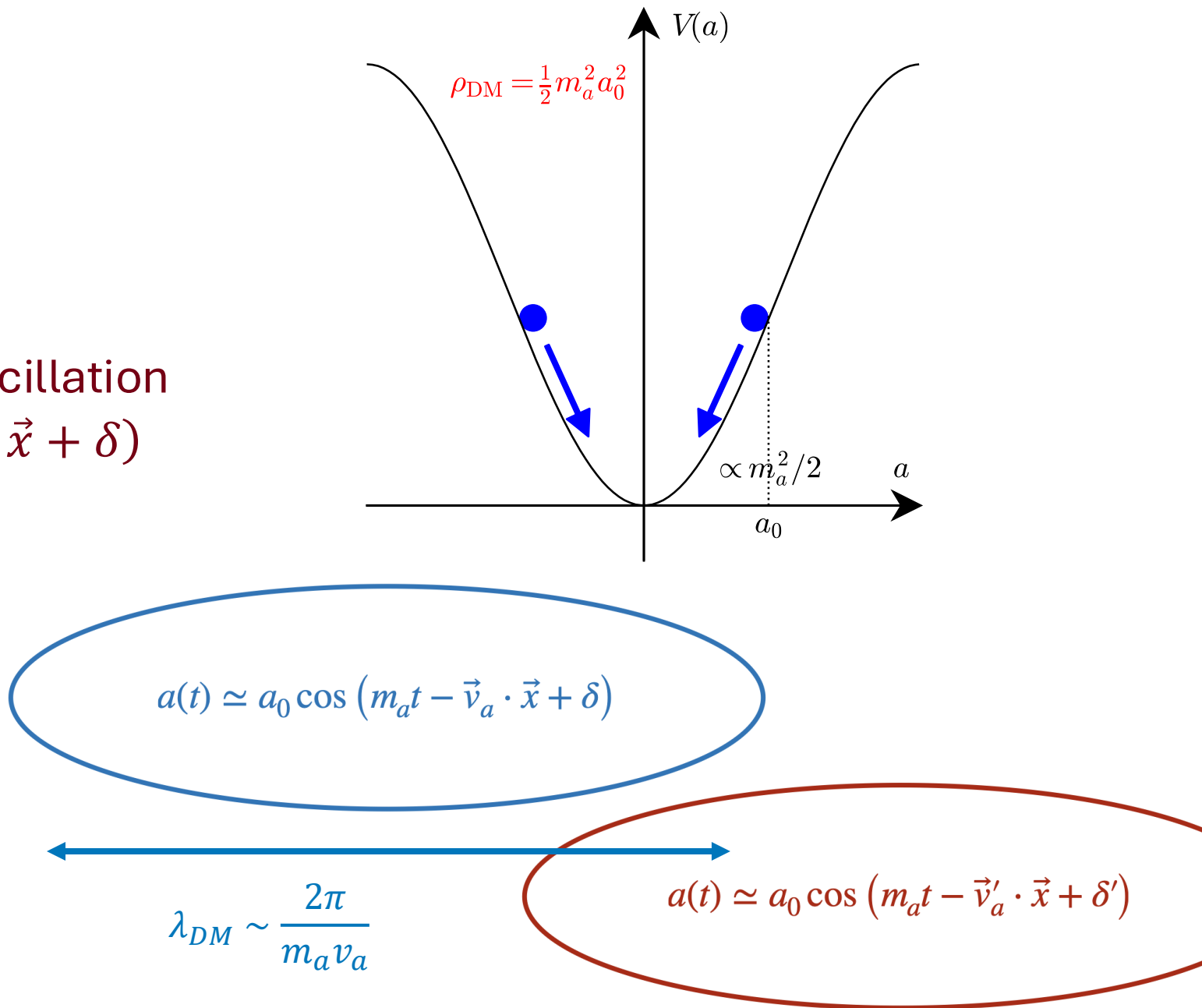
Mass scale of dark matter



- Classical **wave-like** dark matter (axion, dark photon) has $\mathcal{O}(10^{20})$ mass spread

Wave dark matter

- Assumes coherent oscillation:
 - DM energy stored in field oscillation
 - $a(t) = a_0 \sin(m_a t - m_a \vec{v}_a \cdot \vec{x} + \delta)$
 - $\rho_{DM} = \frac{1}{2} m_a^2 a_0^2$
- Coherence time of oscillation
 - $\tau_{DM} \sim \frac{\lambda_{DM}}{v_a} \sim 7s \left(\frac{10^{-10} \text{ eV}}{m_a} \right)$



Wave dark matter signals at direct detection

- Coherent oscillation leaves interaction-dependent signals on direct detection

$$a(t) = a_0 \sin(m_a t - m_a \vec{v}_a \cdot \vec{x} + \delta)$$

Example: axion-fermion interaction

$$\mathcal{L} = \sum_{\chi=e,n,p,\dots} g_{a\chi\chi} \frac{\partial_\mu a}{2m_\chi} \bar{\chi} \gamma^\mu \gamma_5 \chi$$

- Non-relativistic limit of the interaction

$$H_{\text{eff}}^\chi = \frac{g_{a\chi\chi}}{m_\chi} \vec{\nabla} a \cdot \vec{S}_\chi$$

- Can be interpreted as an effective magnetic field acting on fermion spins

$$\gamma_\chi \vec{B}_{\text{eff}}^\chi \simeq \sqrt{2\rho_{DM}} \frac{g_{a\chi\chi}}{e} \vec{v}_{DM} \cos(m_a t + \delta)$$

and similar (but different) interactions for dark photon...

Wave dark matter signals at direct detection

- Coherent oscillation leaves interaction-dependent signals on direct detection

$$a(t) = a_0 \sin(m_a t - m_a \vec{v}_a \cdot \vec{x} + \delta)$$

Example: axion-fermion interaction

$$\mathcal{L} = \sum_{\chi=e,n,p,\dots} g_{a\chi\chi} \frac{\partial_\mu a}{2m_\chi} \bar{\chi} \gamma^\mu \gamma_5 \chi$$

- Non-relativistic limit of the interaction

$$H_{\text{eff}}^{\chi} = \frac{g_{a\chi\chi}}{m_\chi} \vec{\nabla} a \cdot \vec{S}_\chi$$

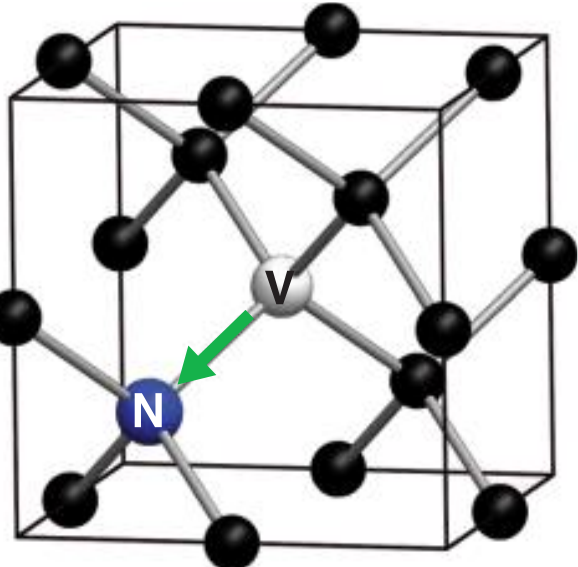
- Can be interpreted as an effective magnetic field acting on fermion spins

$$\gamma_\chi \vec{B}_{\text{eff}}^{\chi} \simeq \sqrt{2\rho_{DM}} \frac{g_{a\chi\chi}}{e} \vec{v}_{DM} \cos(m_a t + \delta)$$

and similar (but different) interactions for dark photon...

① NV center in diamond

(a)



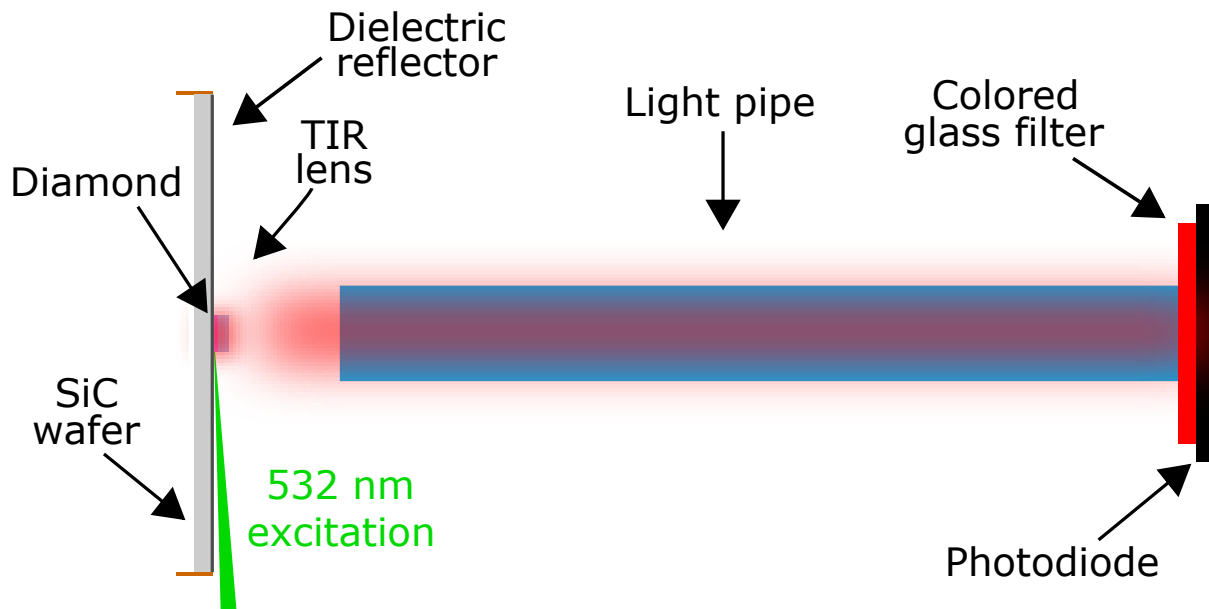
NV II [111]

L. M. Pham '13

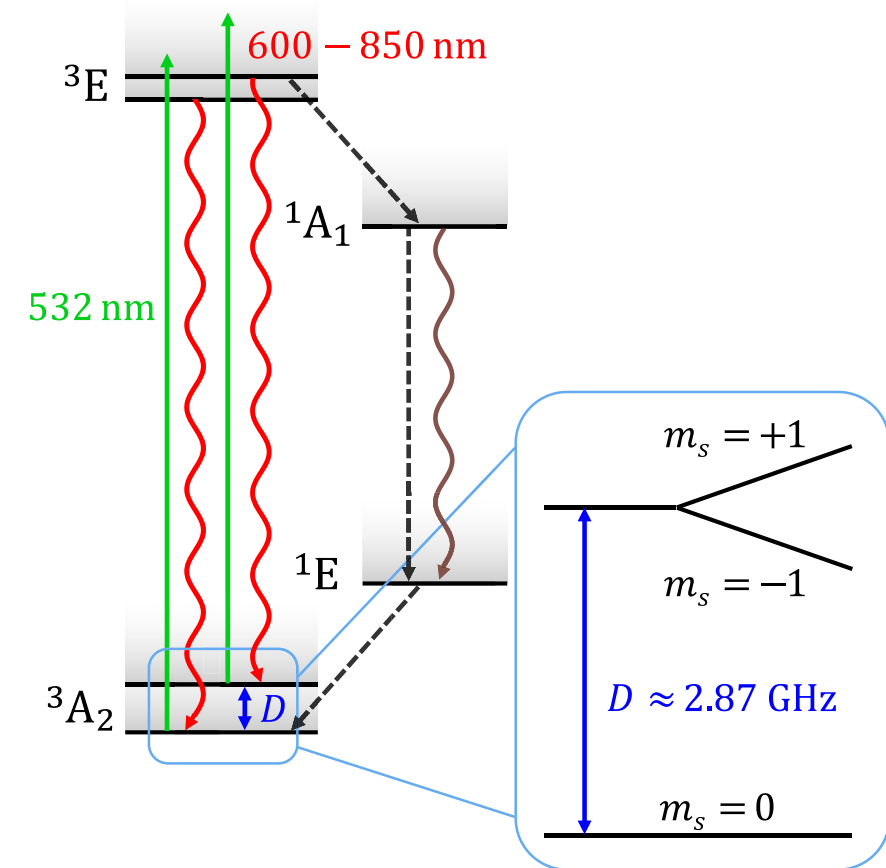


- A stable complex of substitutional nitrogen (N) and vacancy (V) in diamond
- The charged state NV^- has two e^- s localized at V
- The ground state: e^- orbital singlet, spin triplet ($S=1$)

Fluorescence measurement



J. F. Barry, et al. '23



J. M. Schloss, et al. '18

- Fluorescence measurement offers access to the mixing angle of the spin state

$$|\psi\rangle = \cos\frac{\theta}{2} |0\rangle + \sin\frac{\theta}{2} |\pm\rangle$$

Rabi cycle

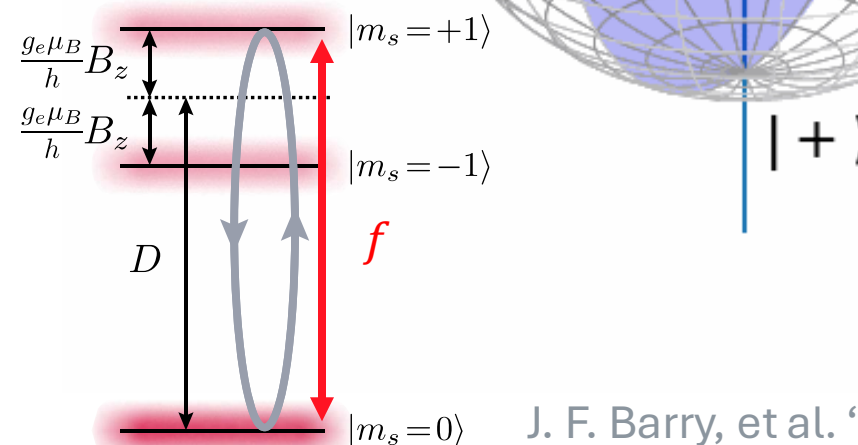
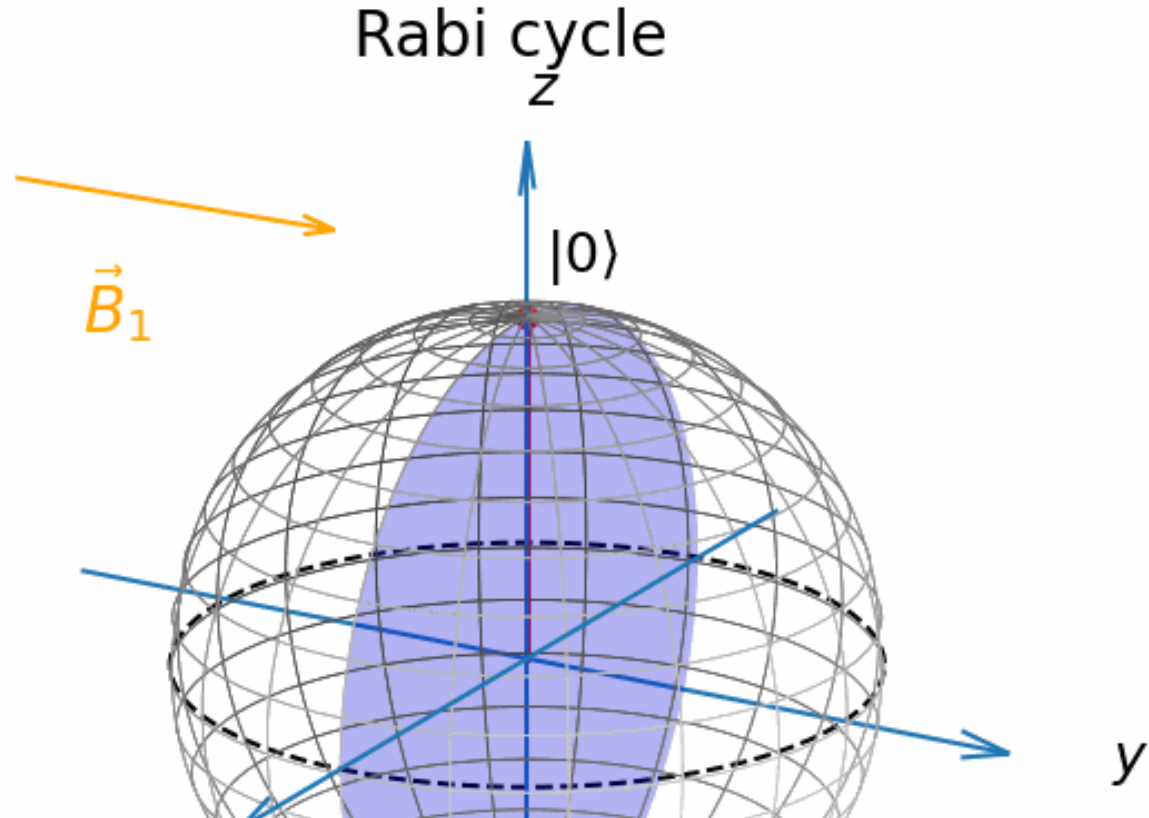
- Spin manipulation by transverse field

$$\vec{B}_1 = B_1 \hat{y} \sin(2\pi f t)$$

- The mixing angle can be controlled

$$|\psi(t)\rangle = \cos\left(\frac{\theta(t)}{2}\right) |0\rangle + \sin\left(\frac{\theta(t)}{2}\right) e^{i\phi} |+\rangle$$
$$\theta(t) = \sqrt{2} \gamma_e B_1 t$$

- Bloch sphere representation maps θ to polar, ϕ to azimuth angles



② Free precession

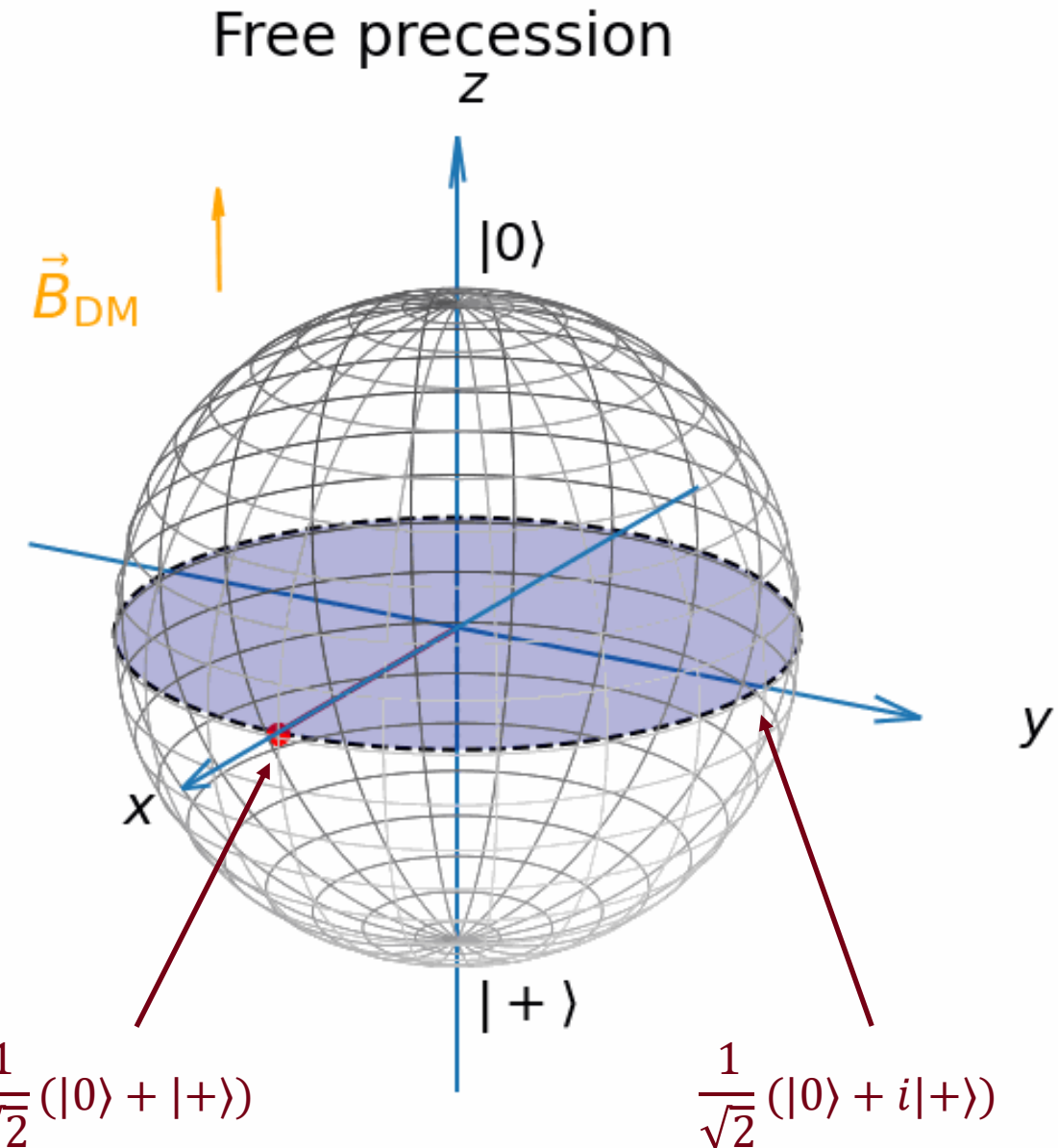
- Prepare the state on the x -axis

$$|\psi(0)\rangle = \frac{1}{\sqrt{2}}(|0\rangle + |+\rangle)$$

- Signal magnetic field B_{DM}^z generates relative phase difference

$$|\psi(\tau)\rangle = \frac{1}{\sqrt{2}}(|0\rangle + e^{i\varphi(\tau)}|+\rangle)$$

$$\varphi(\tau) = \gamma_e \int_0^\tau dt B_{DM}^z(t) \simeq \gamma_e B_{DM}^z \tau$$

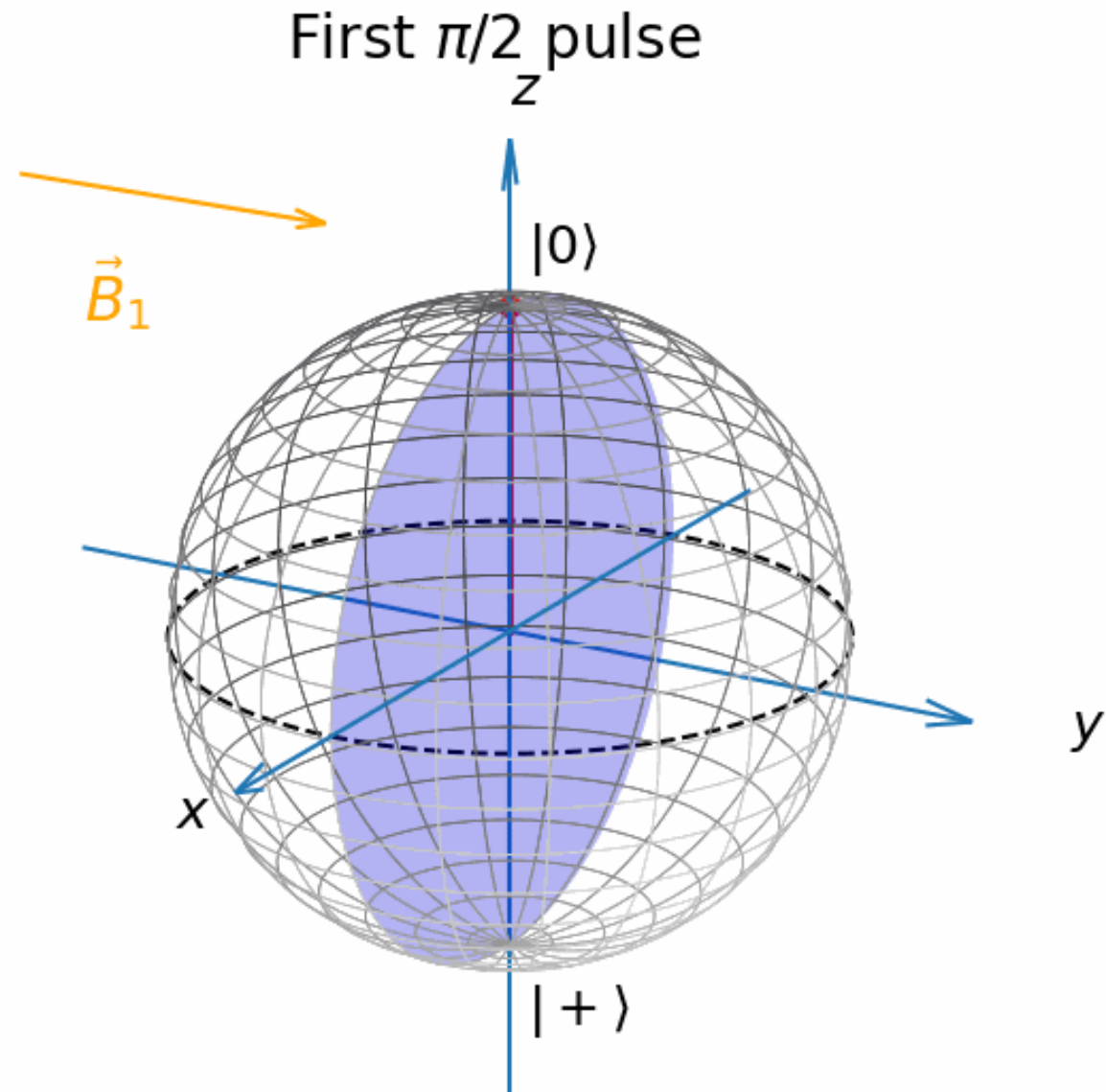


Ramsey sequence

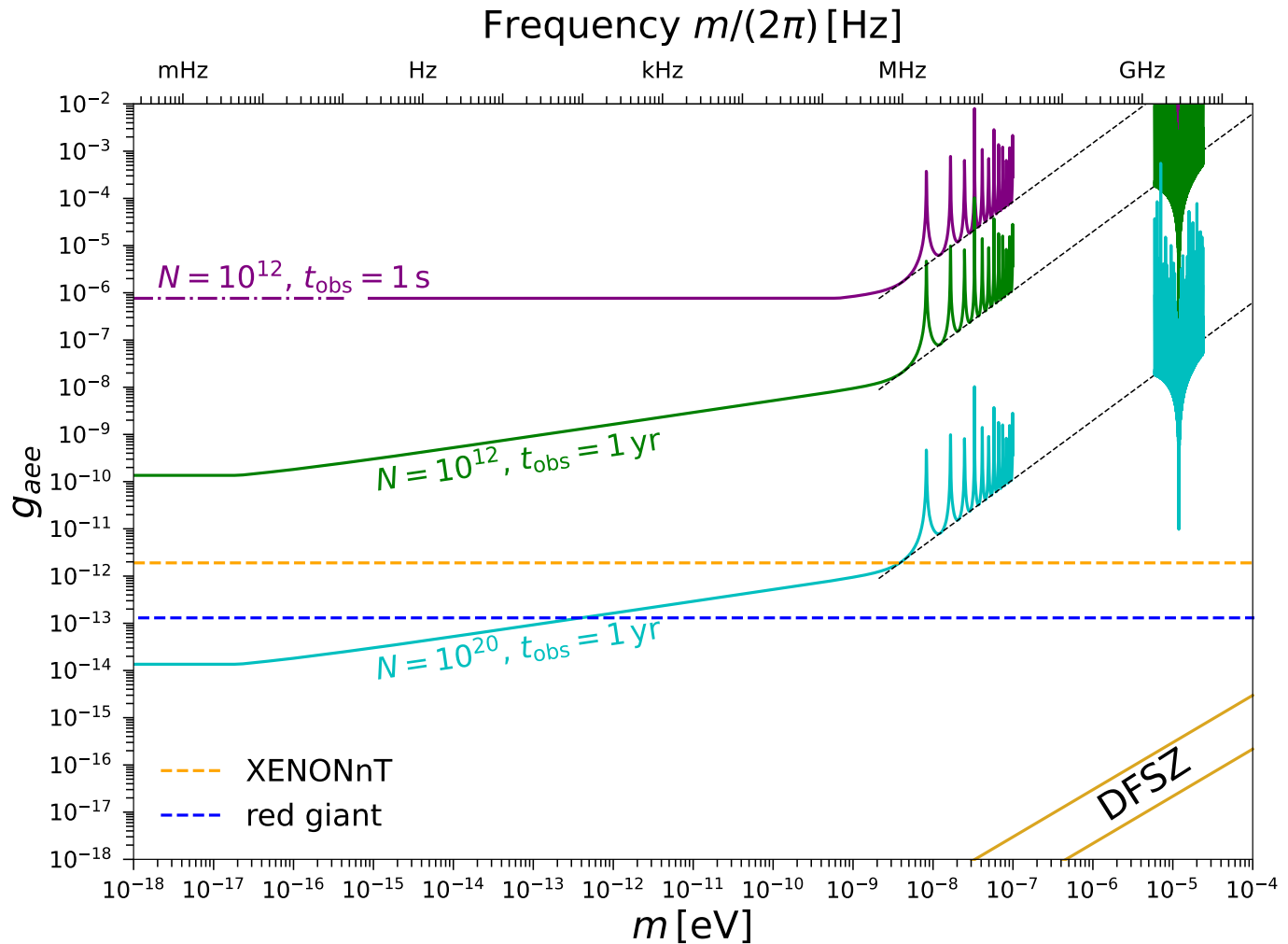
Detection protocol for DC signals

1. $(\pi/2)_y$ pulse
2. Free precession for τ
3. $(\pi/2)_x$ pulse
4. Fluorescence measurement

- Signal estimate $S \equiv \frac{1}{2} \langle \psi_{fin.} | \sigma_z | \psi_{fin.} \rangle \propto \varphi(\tau)$
- $\tau \sim T_2^* \sim 1 \mu s$: spin relaxation (dephasing)



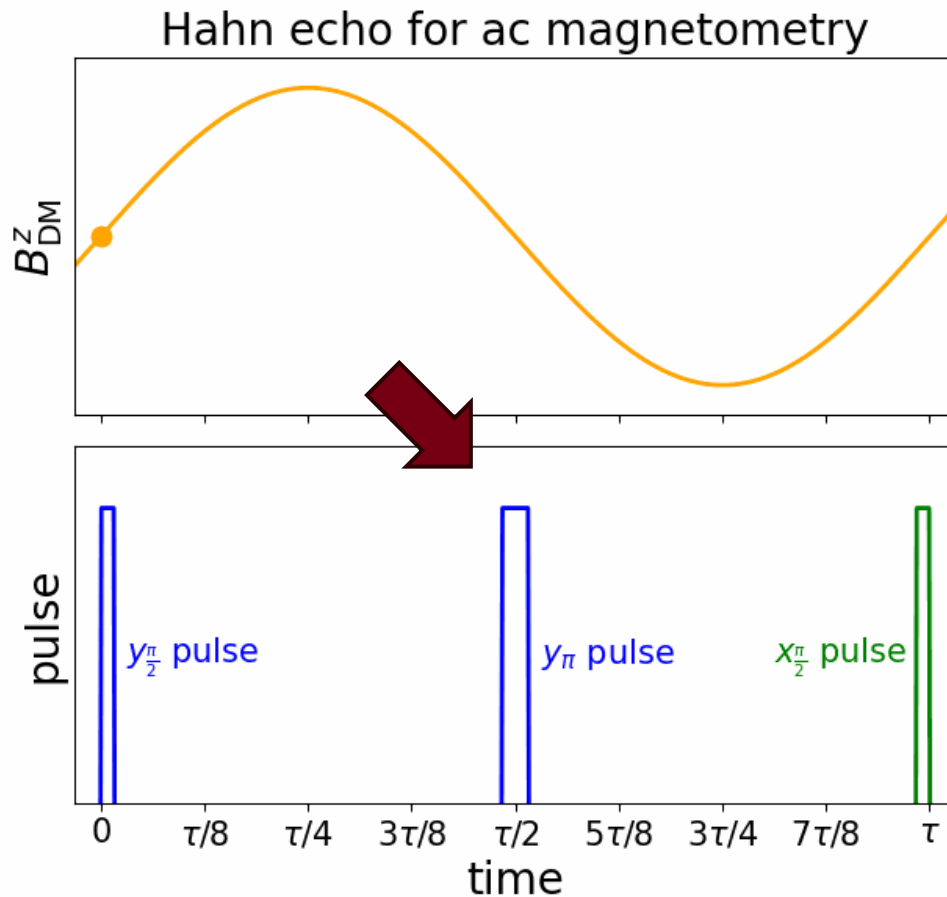
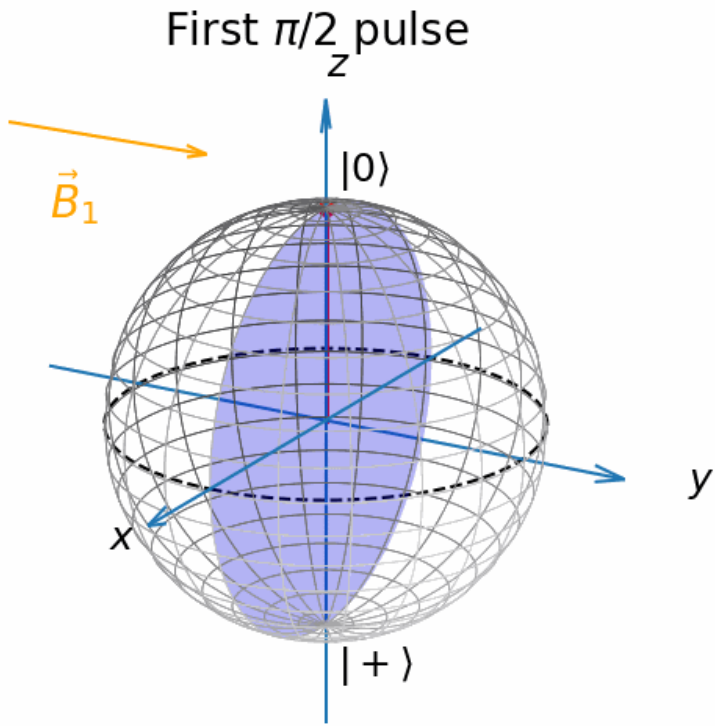
Sensitivity on axion DM (DC)



SC, et al. [2302.12756]

- (Roughly) universal sensitivity to the dc-like region $m < 2\pi/T_2^* \sim 10^{-8} \text{ eV}$

Spin echo sequence for AC signals



- $\varphi(\tau) = \int_0^{\tau/2} dt B_{DM}^z(t) - \int_{\tau/2}^{\tau} dt B_{DM}^z(t)$ is targeted at the frequency $\sim 1/\tau$

Longer relaxation time, dynamical decoupling (DD)

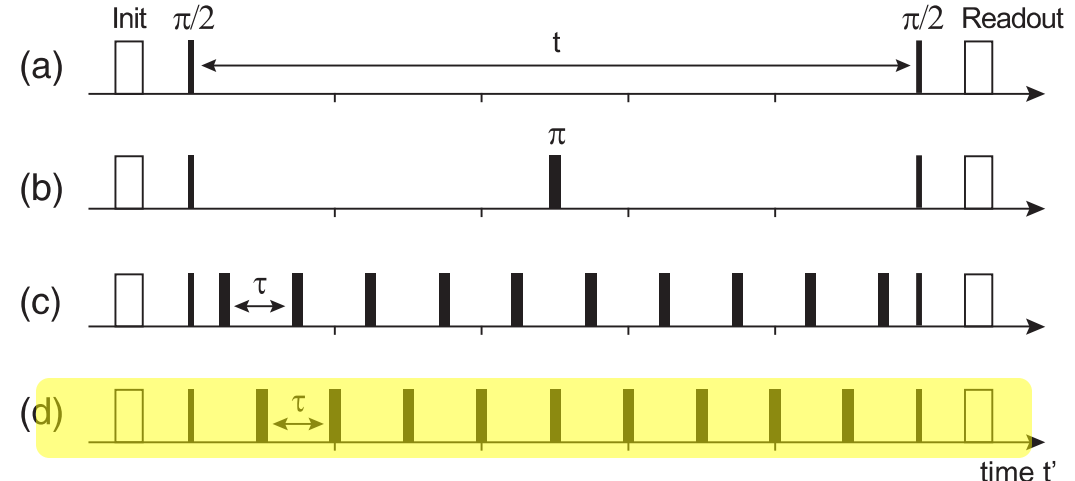
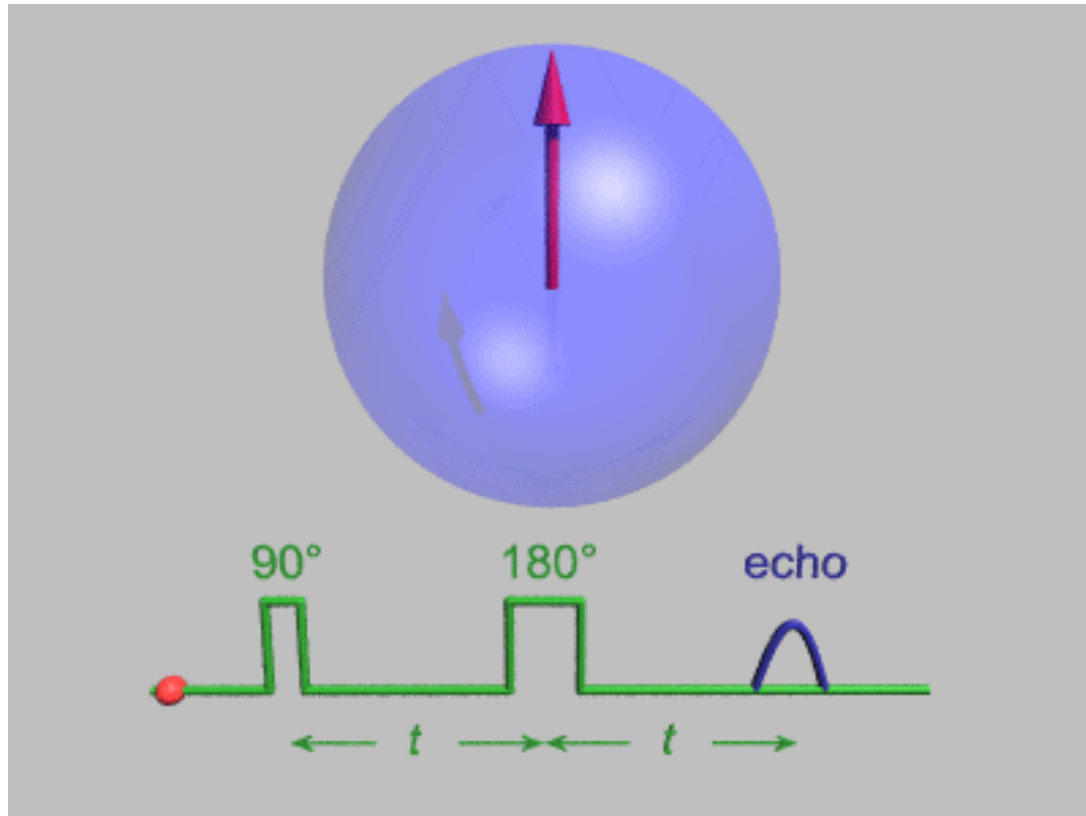


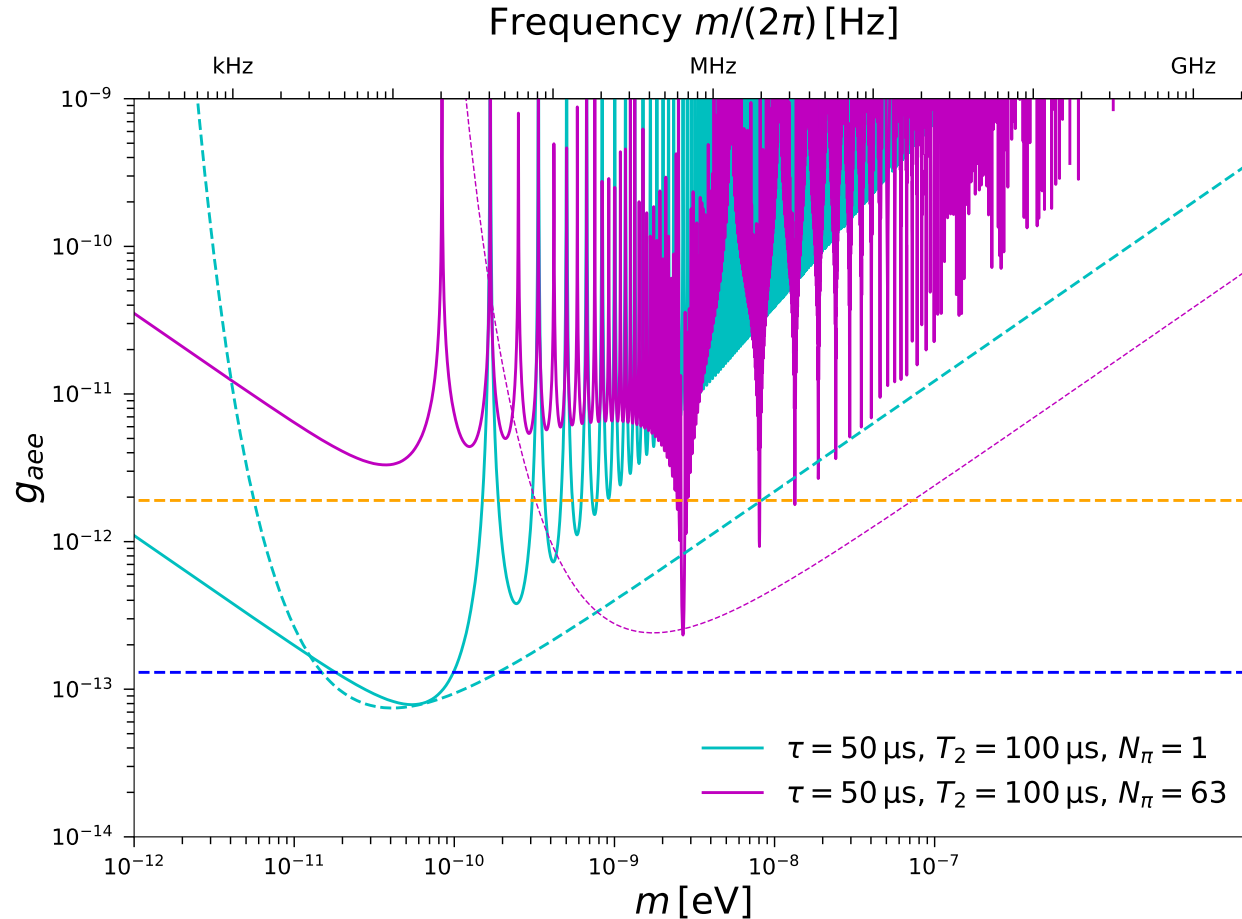
FIG. 5. Pulse diagrams for dc and ac sensing sequences. Narrow blocks represent $\pi/2$ pulses and wide blocks represent π pulses, respectively. t is the total sensing time and τ is the interpulse delay. (a) Ramsey sequence. (b) Spin-echo sequence. (c) Carr-Purcell (CP) multipulse sequence. (d) PDD multipulse sequence.

- No dephasing from dc fields
- Relaxation time $T_2 \sim 100 \mu\text{s} \gg T_2^* \sim 1 \mu\text{s}$

- Even longer T_2 with DD

Degen, et al. “Quantum Sensing” ‘17

Sensitivity on axion DM (Spin echo, DD)



- Pros: better sensitivity at target frequency $\sim N_\pi/T_2 \sim N_\pi \times 10$ kHz
- Cons: (relatively) narrow-band search

③ Full control of nuclear (^{14}N) spins

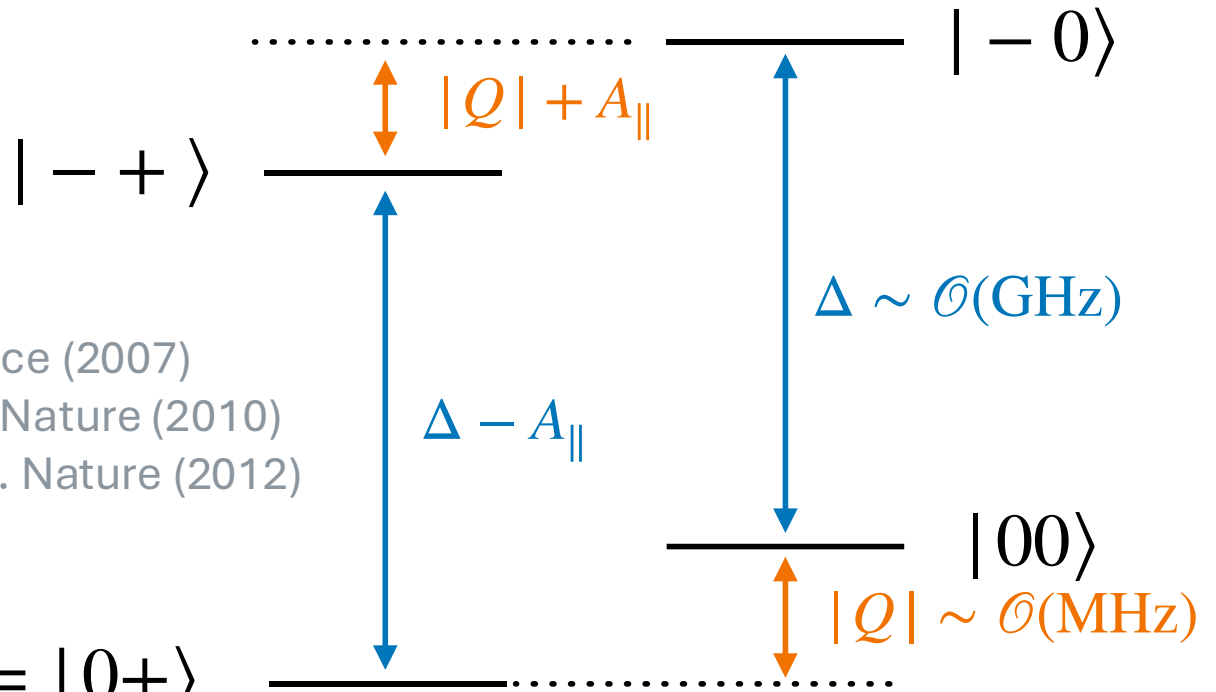
- Hyperfine interaction between e^- and ^{14}N spins ($I = 1$)

$$H_{hyp.} = A_{\parallel} S_z I_z$$

Dutt, et al. Science (2007)
Neumann, et al. Nature (2010)
van der Sar, et al. Nature (2012)

- Causes hyperfine splitting of energy levels

$$|S_z I_z\rangle = |0+\rangle$$



- Full control on two-qubit system of e^- and ^{14}N spins available

Full control of nuclear (^{14}N) spins

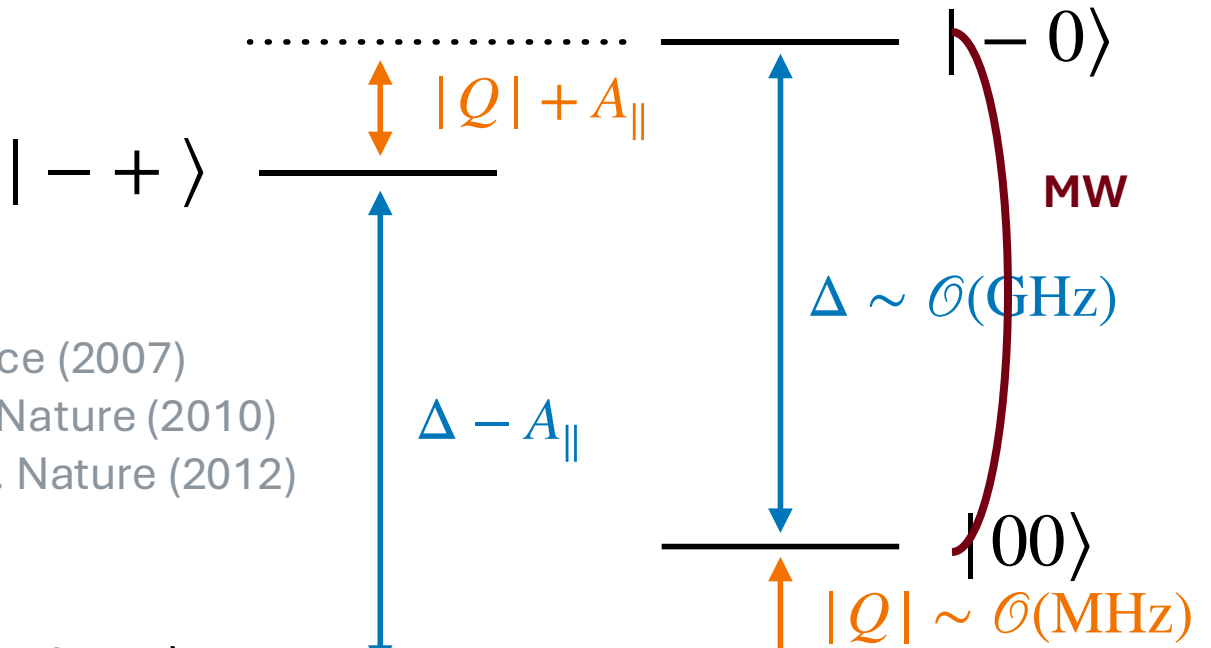
- Hyperfine interaction between e^- and ^{14}N spins ($I = 1$)

$$H_{hyp.} = A_{\parallel} S_z I_z$$

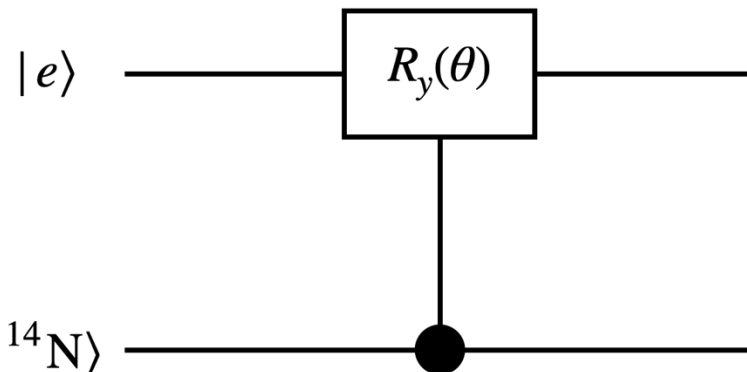
Dutt, et al. Science (2007)
Neumann, et al. Nature (2010)
van der Sar, et al. Nature (2012)

- Causes hyperfine splitting of energy levels

$$|S_z I_z\rangle = |0+\rangle$$



- Full control on two-qubit system of e^- and ^{14}N spins available



Full control of nuclear (^{14}N) spins

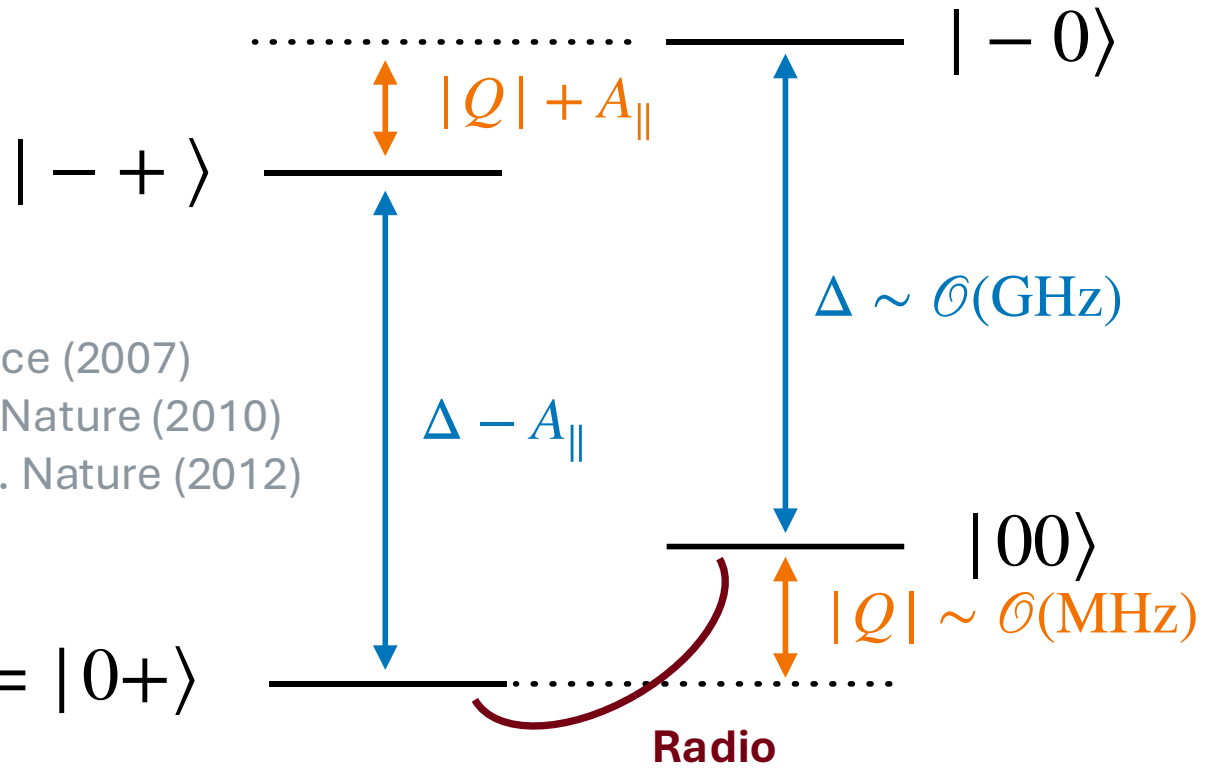
- Hyperfine interaction between e^- and ^{14}N spins ($I = 1$)

$$H_{hyp.} = A_{\parallel} S_z I_z$$

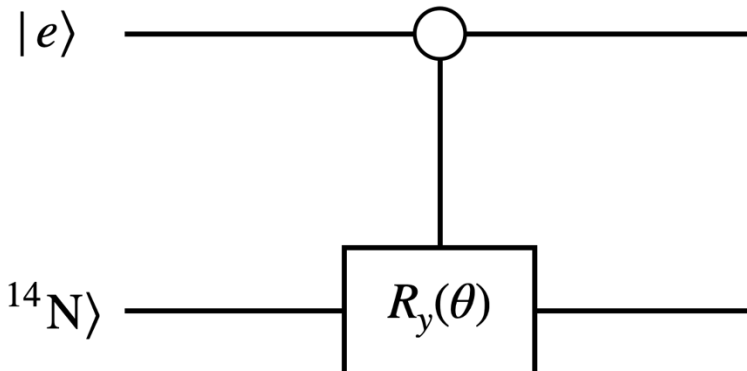
Dutt, et al. Science (2007)
Neumann, et al. Nature (2010)
van der Sar, et al. Nature (2012)

- Causes hyperfine splitting of energy levels

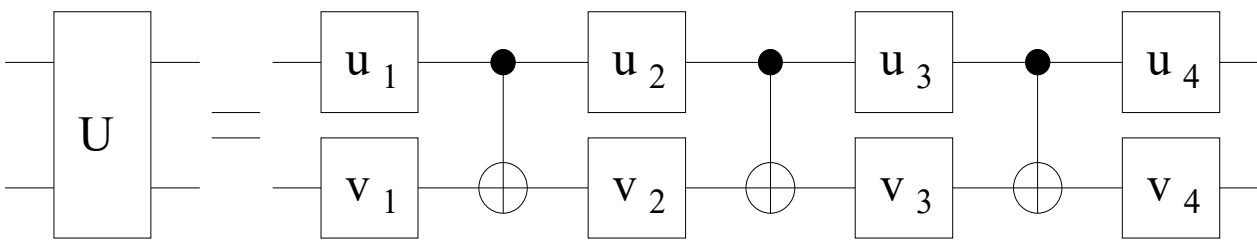
$$|S_z I_z\rangle = |0+\rangle$$



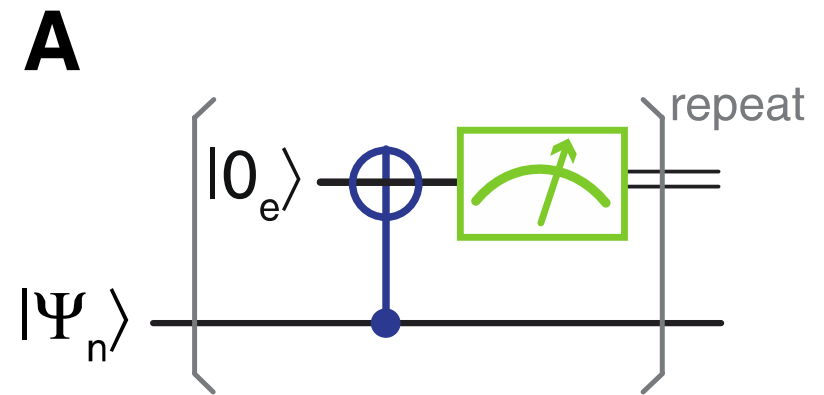
- Full control on two-qubit system of e^- and ^{14}N spins available



General manipulation and read out



Vidal & Dawson, PRA (2003)



Neumann, et al. Nature (2010)

- General $SU(4)$ with ≤ 3 CNOT gates

- Precise measurement possible

Axion interaction with ^{14}N spin

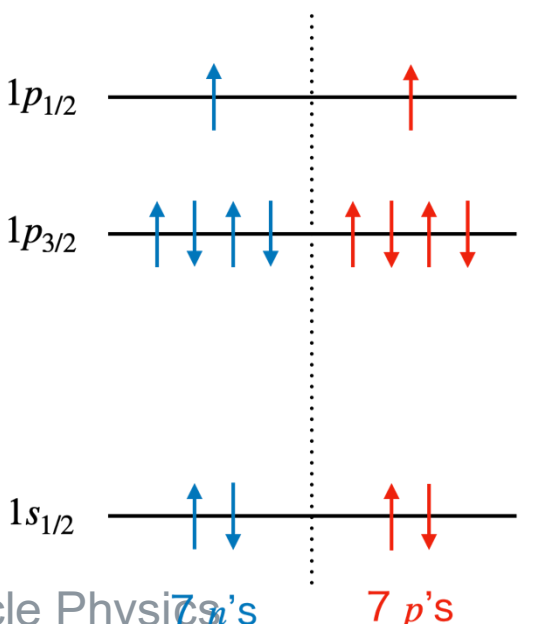
“Introductory Nuclear Physics” by K. S. Krane

- Axion interactions with
 - Orbital angular momentum: None
 - Neutron spins $\propto g_{ann}$
 - Proton spins $\propto g_{app}$
- Need to understand composition of ^{14}N spin

$$H_{int} = \gamma_{^{14}N} \vec{B}_a \cdot \vec{I}$$

$$\vec{B}_a \propto \frac{1}{6} \left(\frac{g_{ann}}{m_n} + \frac{g_{app}}{m_p} \right)$$

$$\equiv \frac{1}{3\tilde{f}_a}$$



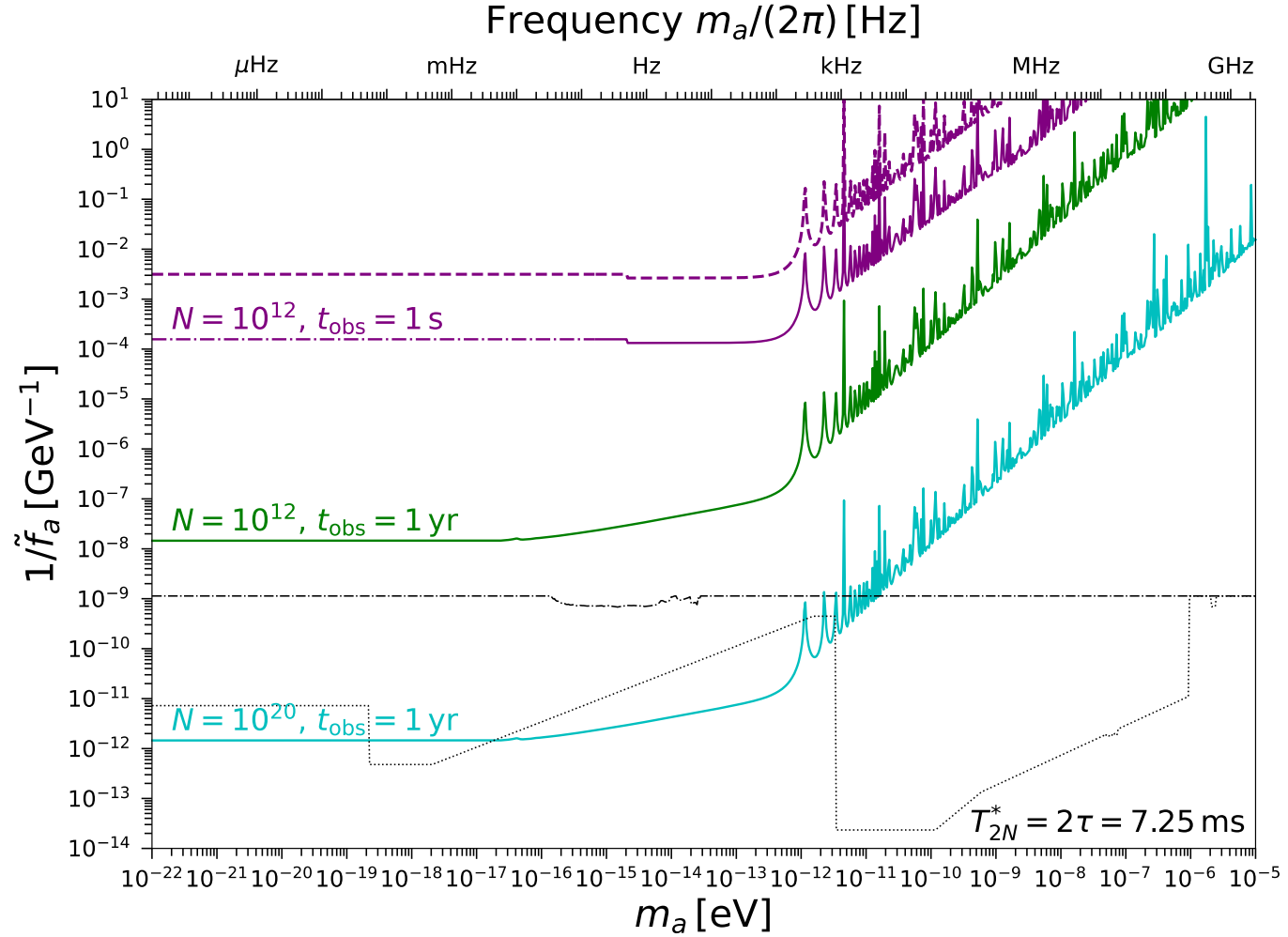
So Chigusa @ The Frontier of Particle Physics

N	ℓ	Harmonic Oscillator		Spin-Orbit Potential	
		Specroscopic Notation	Spin-orbit	\mathcal{D}	Magic Number
6	0	4s	1i _{1/2}	;	58 184
	2	3d	1i _{3/2}		
	4	2g	3p _{1/2}		
	6	1f	3p _{3/2}		
5	1	3p	2f _{5/2}	44 126	
	3	2f	2f _{7/2}		
	5	1h	1h _{9/2}		
4	0	3s	1h _{11/2}	32 82	
	2	2d	2d _{3/2}		
	4	1g	2d _{5/2}		
3	1	2p	1g _{7/2}	22 50	
	3	1f	1g _{9/2}		
	1		2p _{1/2}		
	3		1f _{5/2}		
	1		2p _{3/2}		
2	0	2s	1f _{7/2}	8 28	
	2	1d	1d _{3/2}		
	0		2s _{1/2}		
	2		1d _{5/2}		
1	1	1p	1p _{1/2}	6 8	
	1		1p _{3/2}		
0	0	1s	1s _{1/2}	2 2	

7 p's

1s's

Sensitivity on axion-nucleon couplings



SC, et al. [2407.07141]

- Benefits from a long coherence time $T_{2N}^* \sim 7 \text{ ms}$

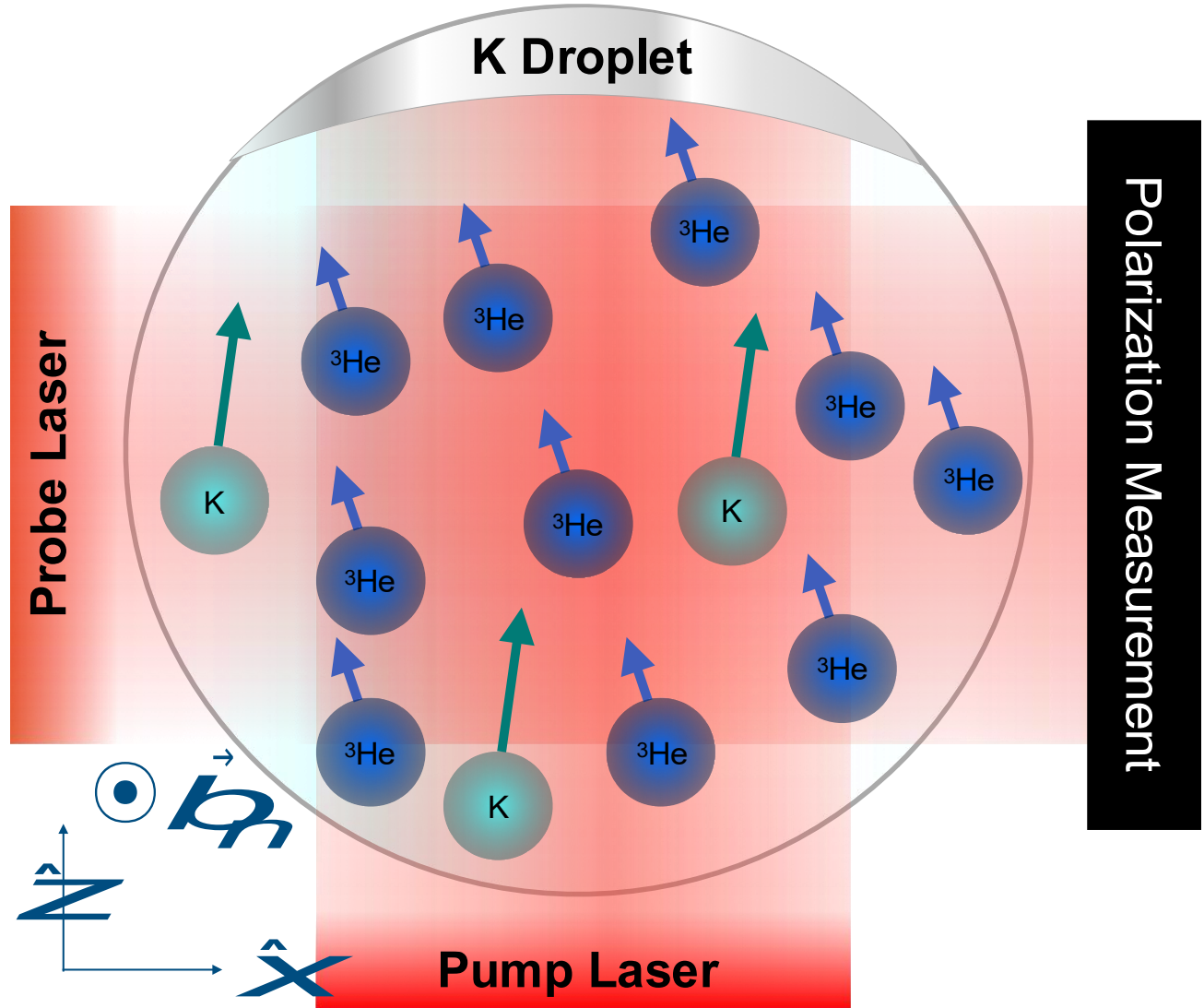
④ Recap: comagnetometry

- Comagnetometry
 - Provides noise mitigation using two spin species
 - Suitable for probing exotic spin interaction like axion

• Ex) Mixed gas of K- ${}^3\text{He}$

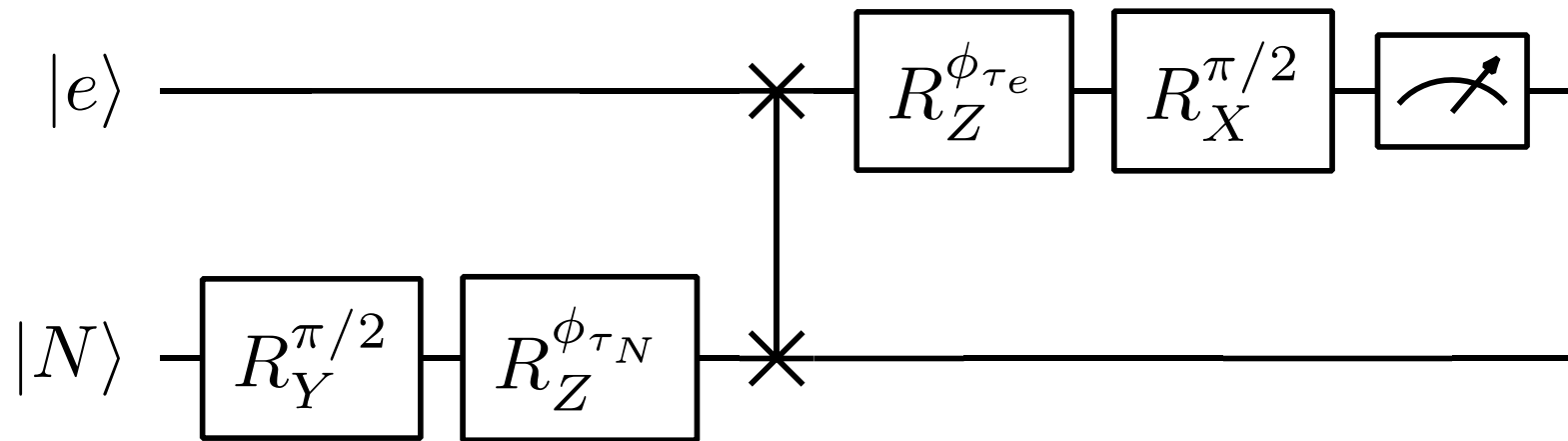
T. W. Kornack and M. V. Romalis '02
G. Vasilakis, et al. '08
J. M. Brown, et al. '10
J. Lee, et al. '18

and more



I. Bloch, et al. JHEP (2020) 167

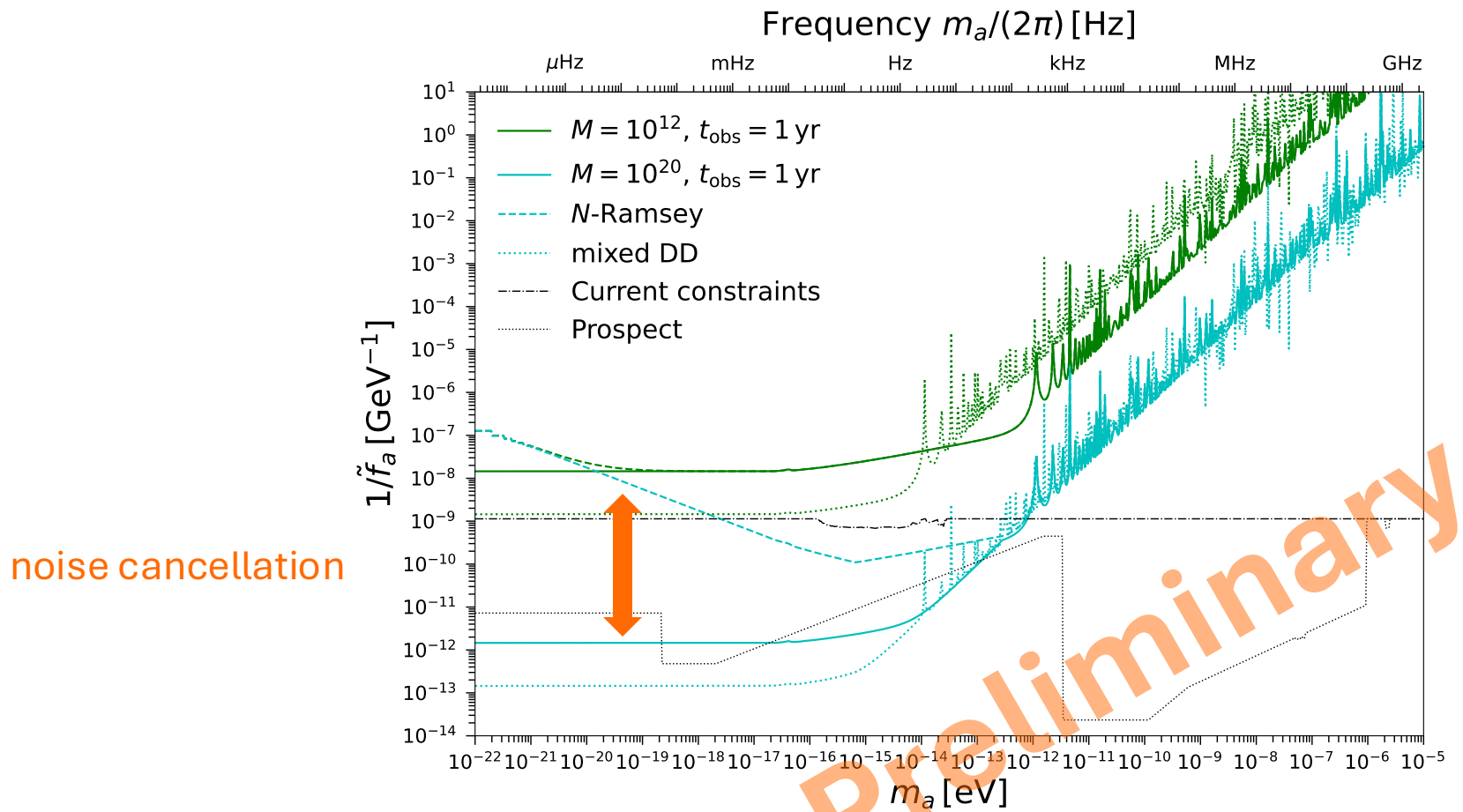
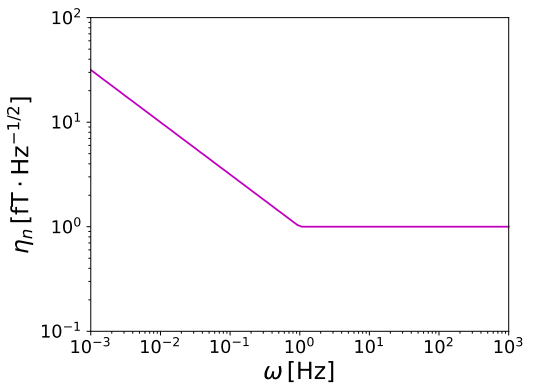
Comagnetometry protocol



- Fine-tuned choice of free precession times lead to noise cancellation
 - $\varphi_{\text{fin.}} = \phi_{\tau_N} + \phi_{\tau_e} \simeq \gamma_e B^z \tau_N + \gamma_N B^z \tau_e$ requires $\frac{\tau_N}{\tau_e} = \left| \frac{\gamma_e}{\gamma_N} \right|$
- Axion signal remains the same order
 - $\varphi_{\text{fin.}} \propto \frac{g_{aee}}{m_e} B_{DM}^z \tau_e + \frac{1}{6} \left(\frac{g_{ann}}{m_n} + \frac{g_{app}}{m_p} \right) B_{DM}^z \tau_N$

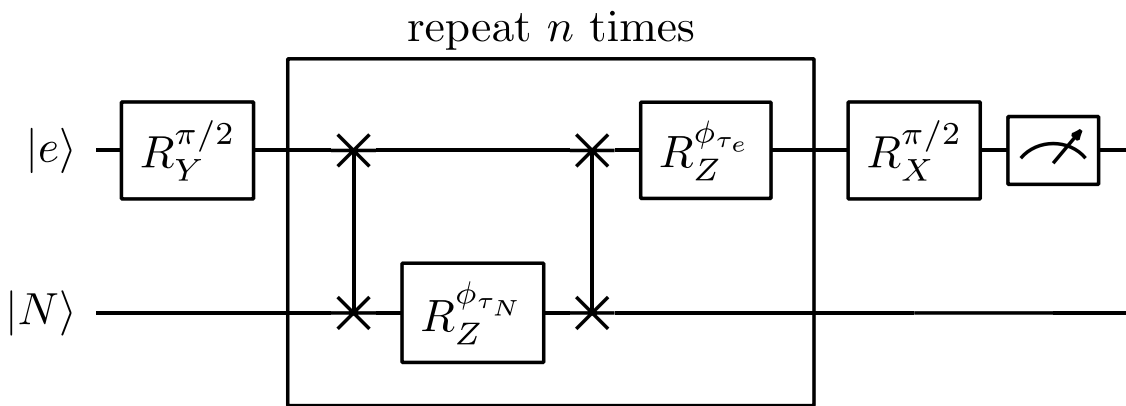
Sensitivity recovery by comagnetometry

- Assumed a white noise + $1/f$ (pink) noise

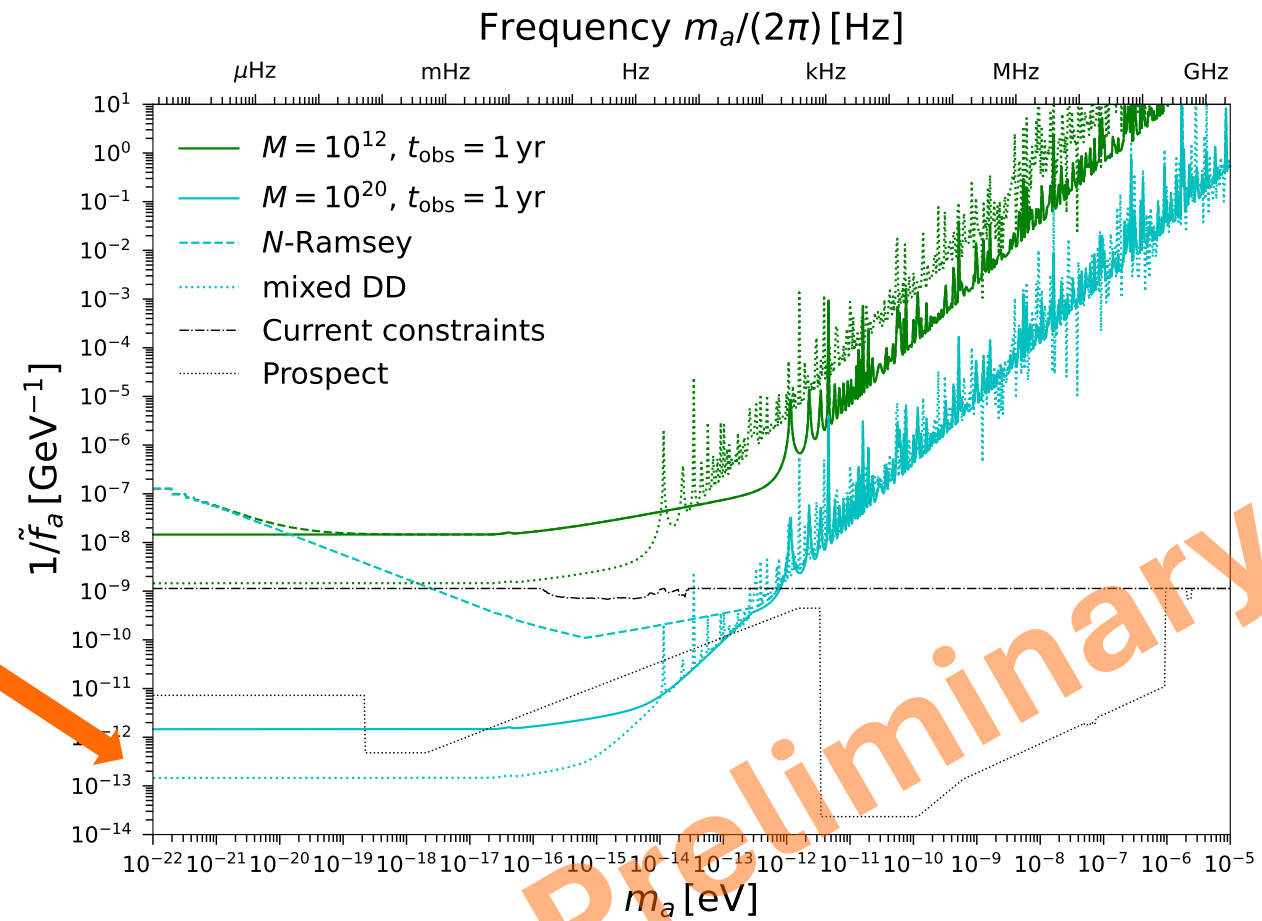


Sensitivity improvement by hybrid DD

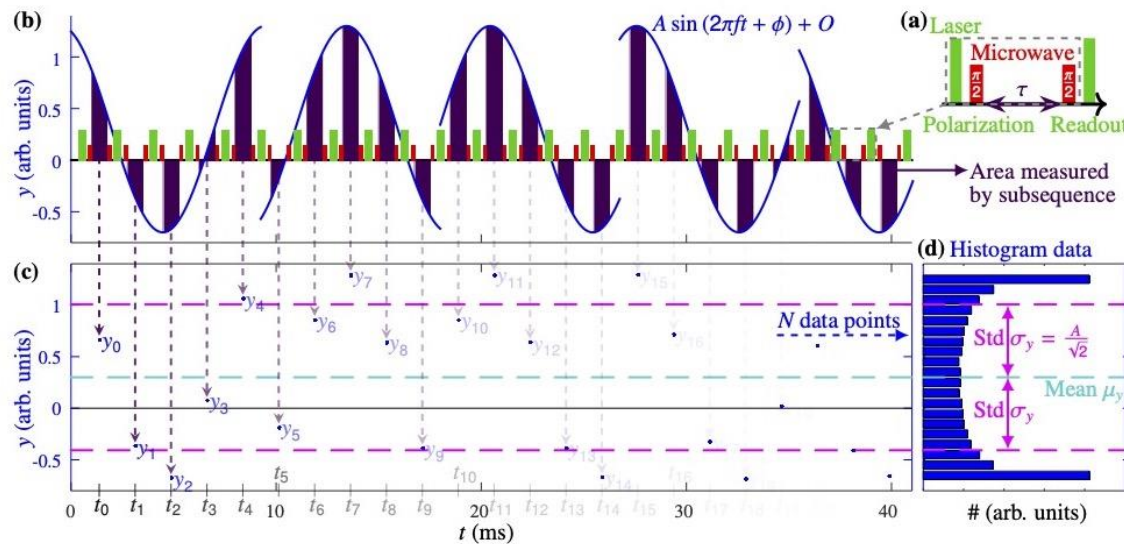
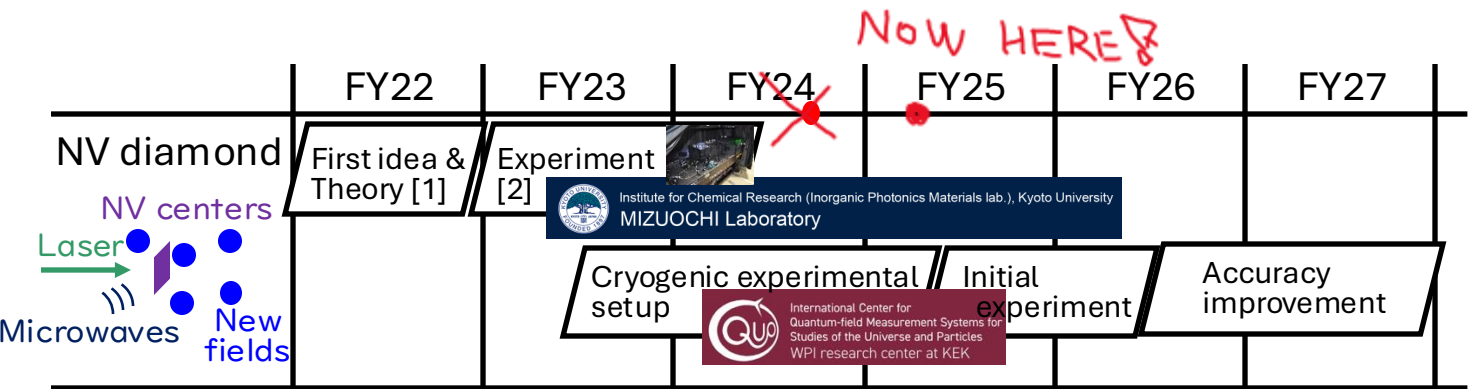
- Realize DD-like sequence with both e^- and ^{14}N spins



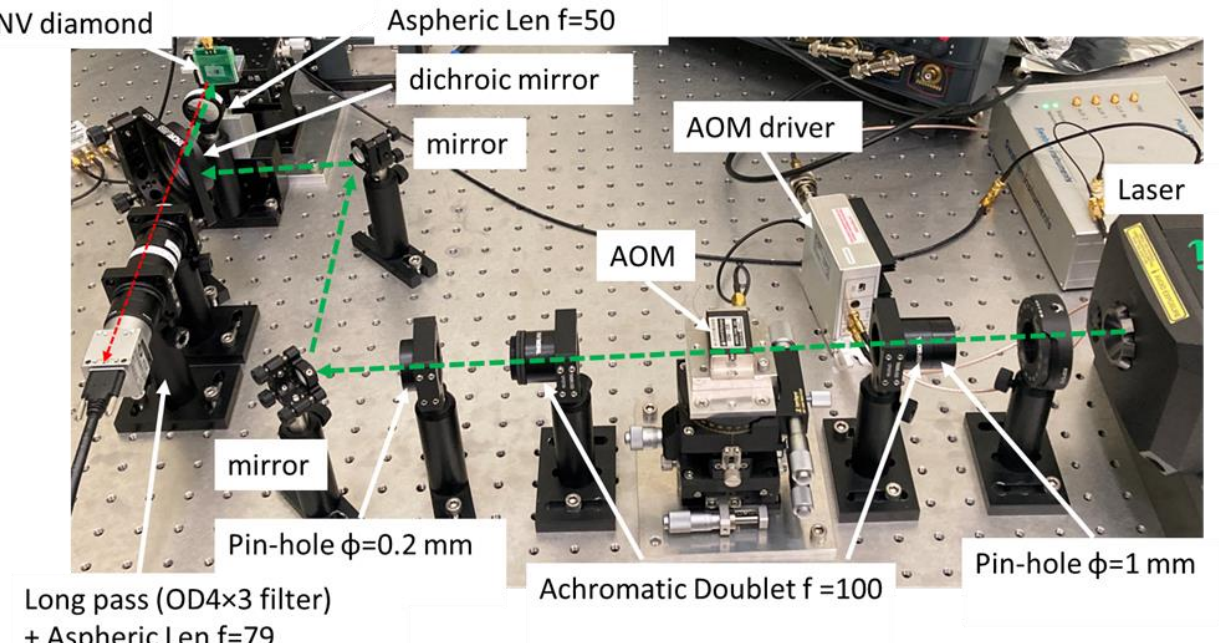
- Pros: longer relaxation time as for DD
- Pros: broad-band search of axion signal
- Need more detailed (experimental) studies to determine relaxation time



Our experiment



Our approach on statistical treatment:
“Standard deviation quantum sensing”
E. D. Herbschleb, SC, et al. [APL Quantum 1, 046106]



Experimental setups @ QUP/KEK (Image credit: Prof. Iizuka)

Discussions and Conclusion

- NV center magnetometry provides opportunities to explore DM signals
 - Over broad frequency range
 - Through various different spins
- DM-specific protocols can be considered for further development
 - Nuclear spins
 - Comagnetometry
 - Hybrid dynamical decoupling for broadband sensing
- Setting up an experiment at QUP with NV + cryogenic

Backup slides

Data analysis with PSD

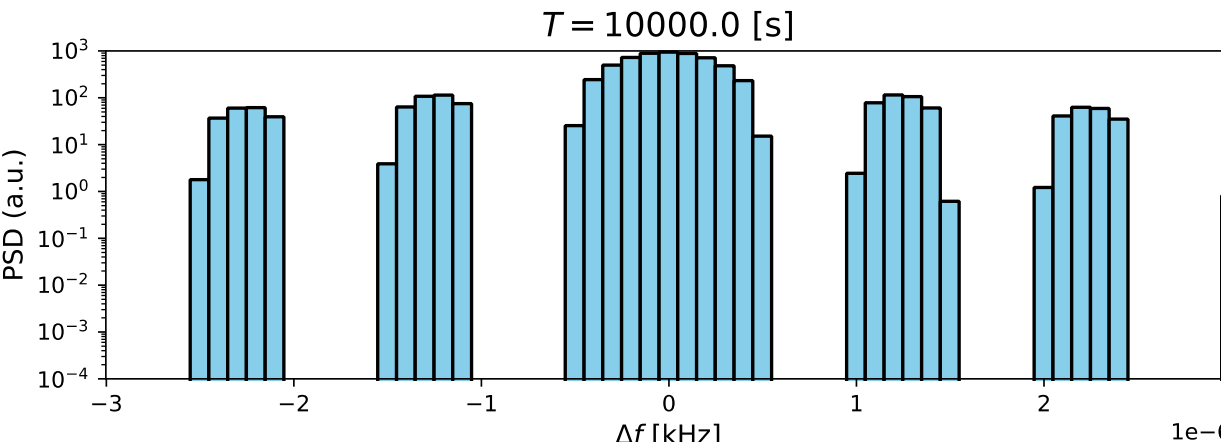
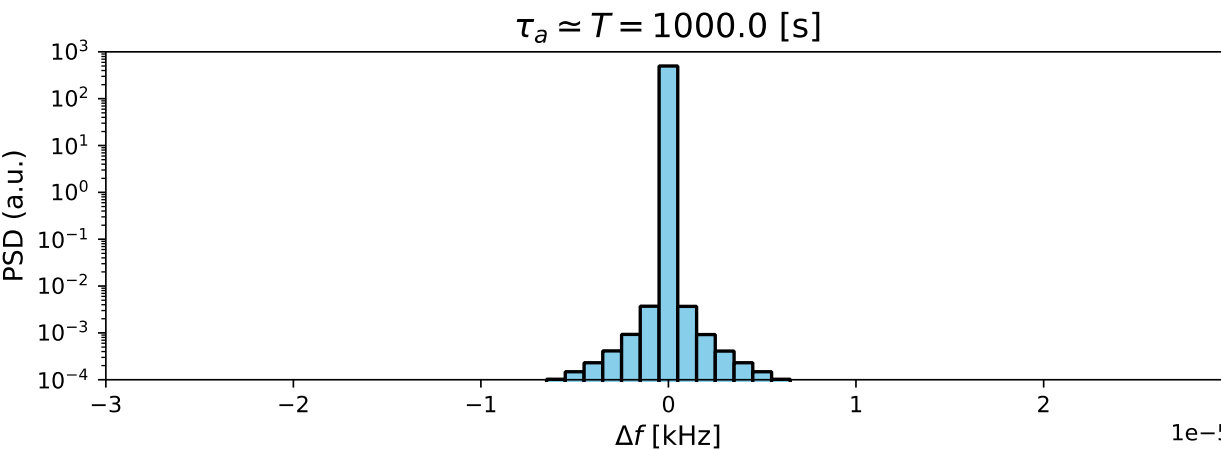
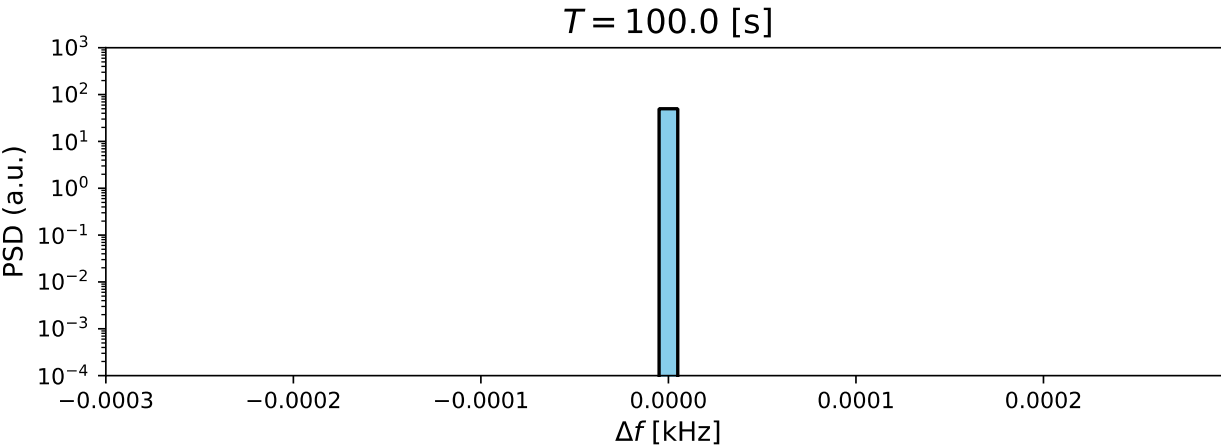
- Dataset $\{S(t_j)\}_{j=1,\dots,N}$ for repeated meas.
- Power spectral density (PSD)

$$P_k \equiv \frac{1}{t_{\text{obs}}} \int dt dt' e^{\frac{i\omega_k(t-t')}{N}} \langle S(t)S(t') \rangle$$
$$\omega_k \equiv \frac{2\pi k}{N\tau} \quad (k = 0, \dots, N-1)$$

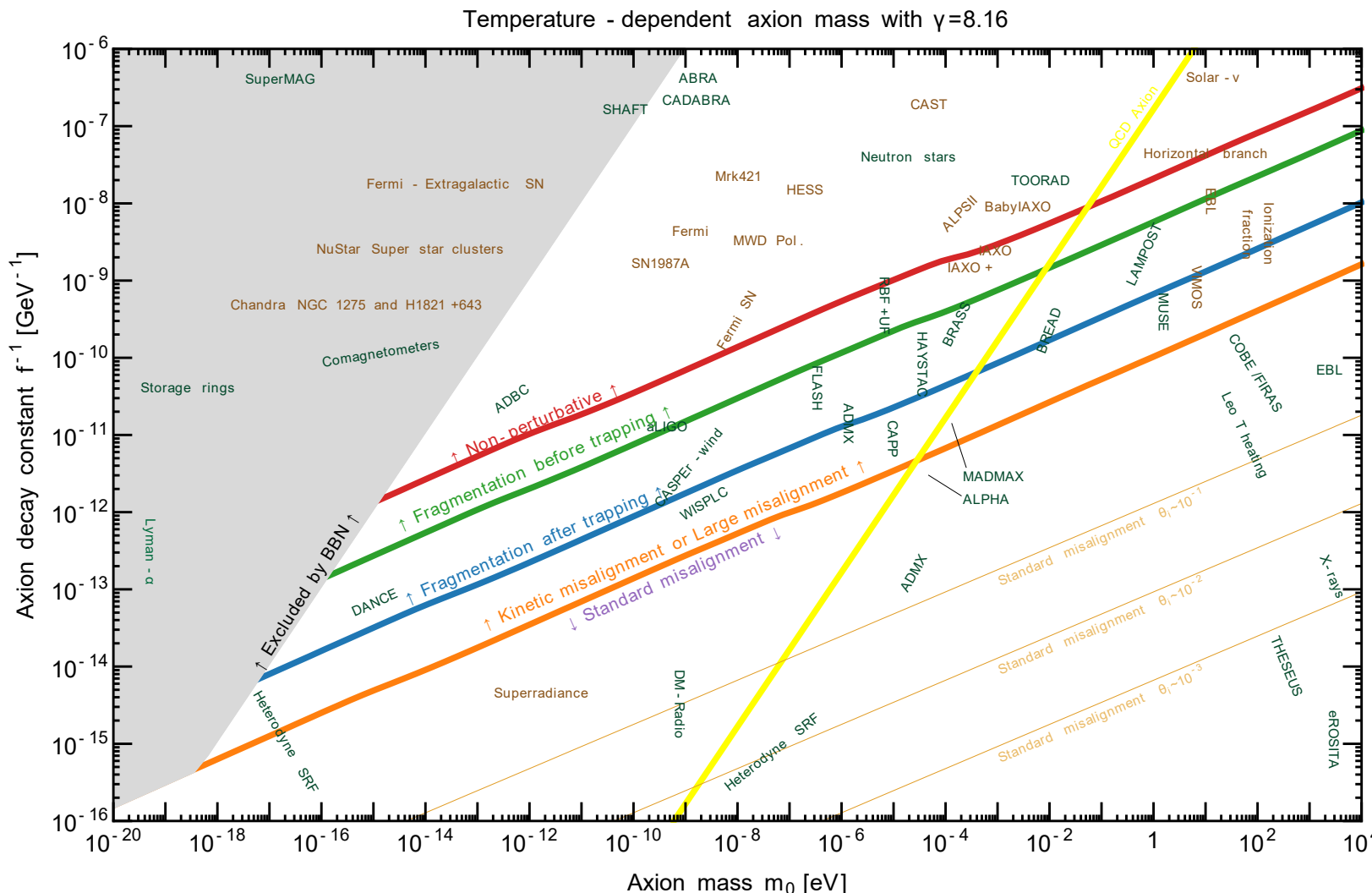
$$\bullet P_k = S_k + \left(B_k = B_k^{\text{proj}} + B_k^{\text{shot}} + B_k^{\text{ext.}} + \dots \right)$$

$$q = 2 \sum_k \left[\left(1 - \frac{B_k}{S_k + B_k} \right) - \ln \left(1 + \frac{S_k}{B_k} \right) \right] \simeq -2.71$$

95% exclusion limit

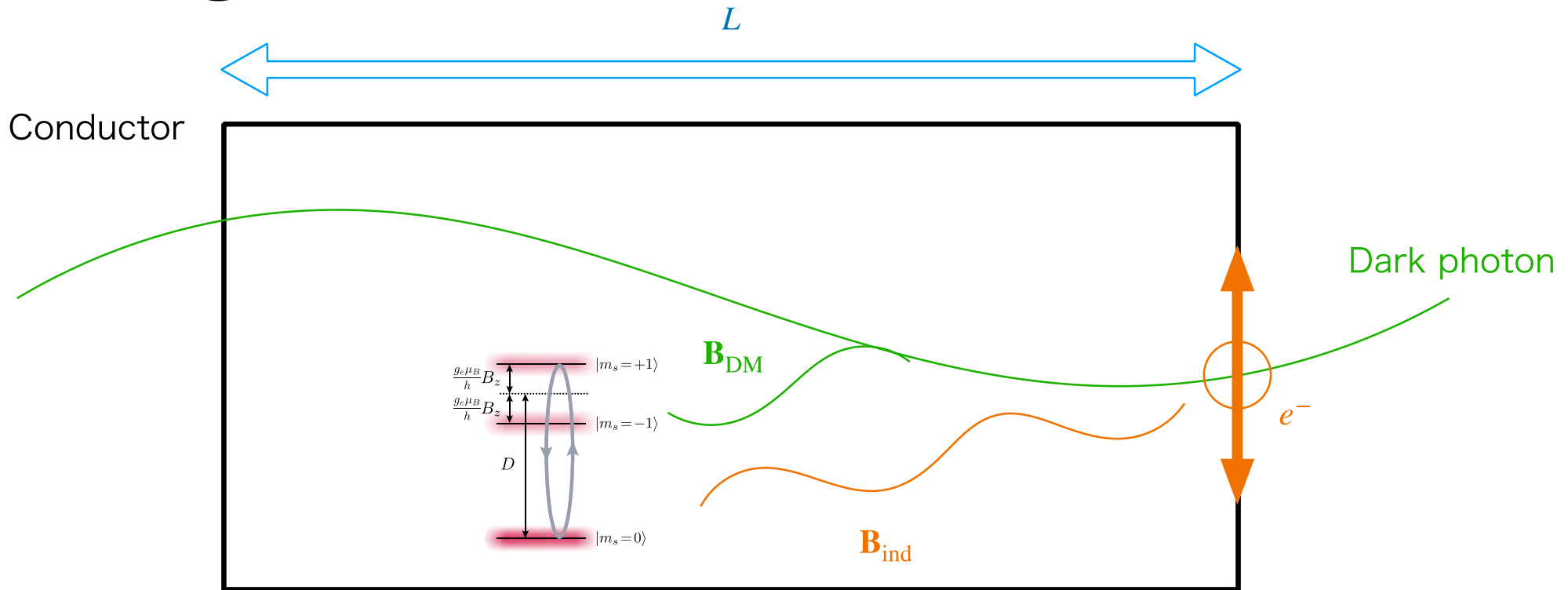


Axion DM parameter space



Eröncel+ [2206.14259]

Shielding effect

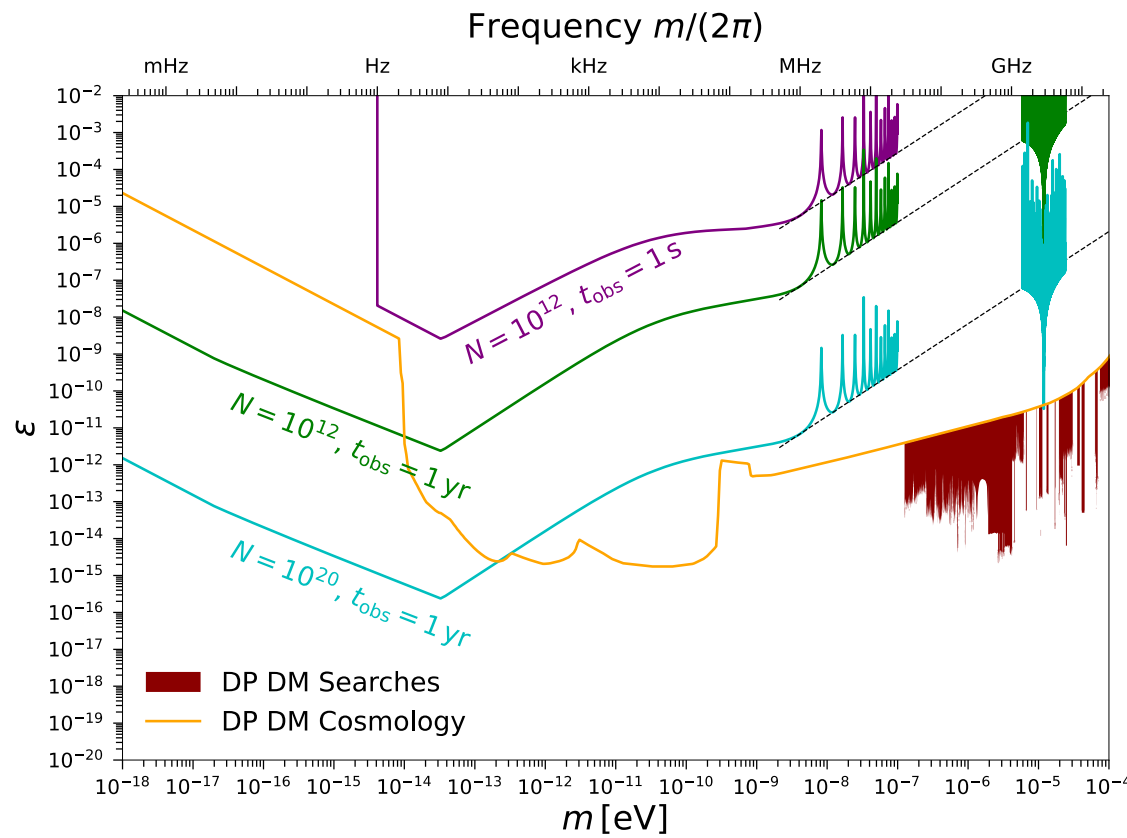


- Electric interaction of the dark photon creates current in the conductor and induces a magnetic field \mathbf{B}_{ind}
- The effective magnetic field may be canceled and “shielded” if $\lambda_{\text{DM}} > L$

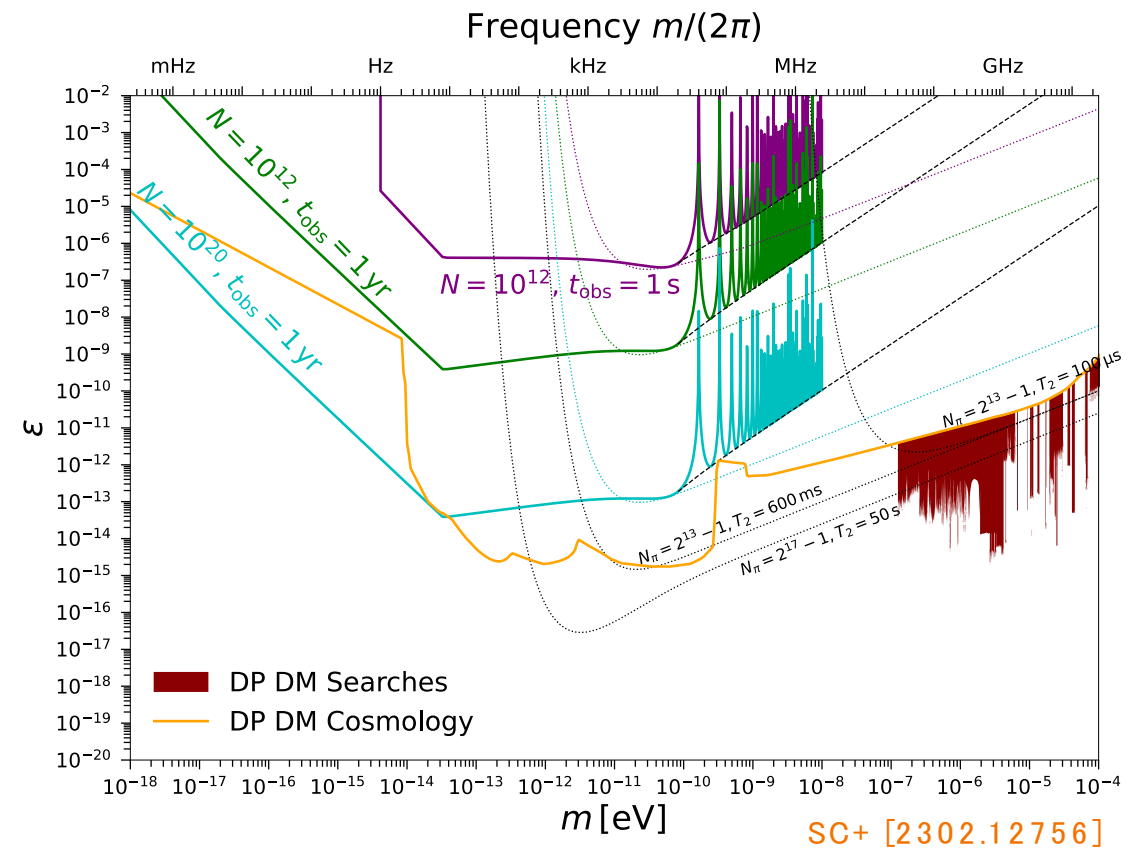
S. Chaudhuri+ [1411.7382] “DM Radio” paper

Sensitivities on dark photon DM

- DC magnetometry



- AC magnetometry



Axion- ^{14}N interaction

- A little algebra of spin synthesis

$$(2_{1/2} \otimes 3_1) \otimes (2_{1/2} \otimes 3_1)$$

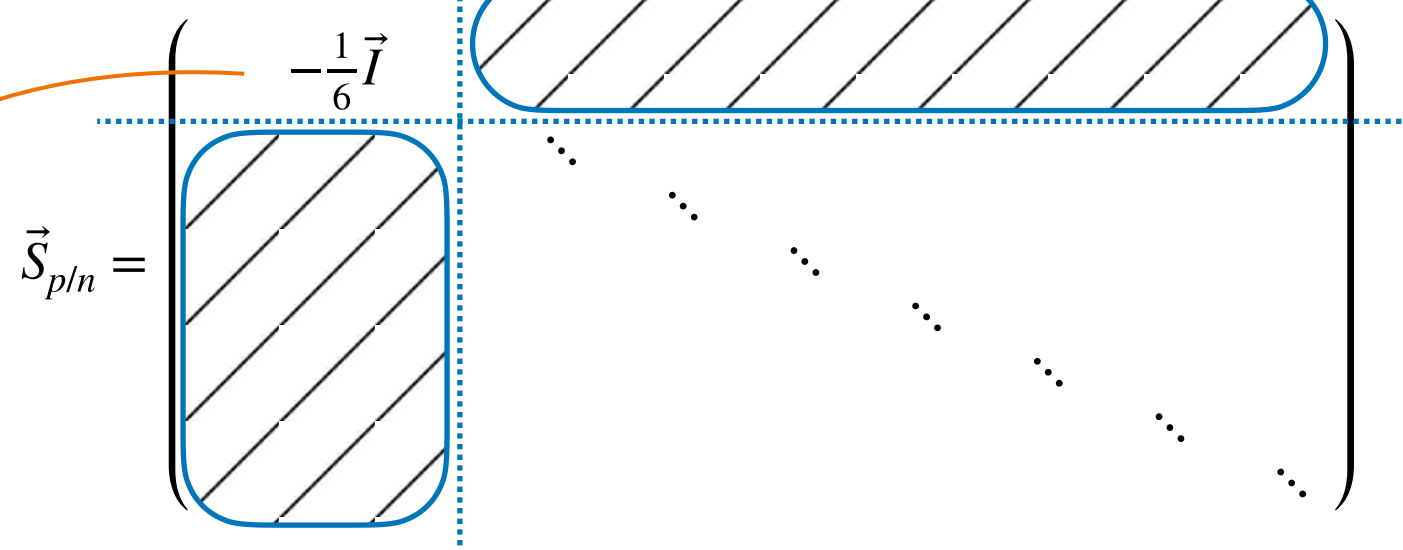
$$= (2_{1/2} \oplus 4_{3/2}) \otimes (2_{1/2} \oplus 4_{3/2})$$

$$= (1_0 \oplus 3_1) \oplus (3_1 \oplus 5_2) \oplus (3_1 \oplus 5_2) \oplus (1_0 \oplus 3_1 \oplus 5_2 \oplus 7_3)$$

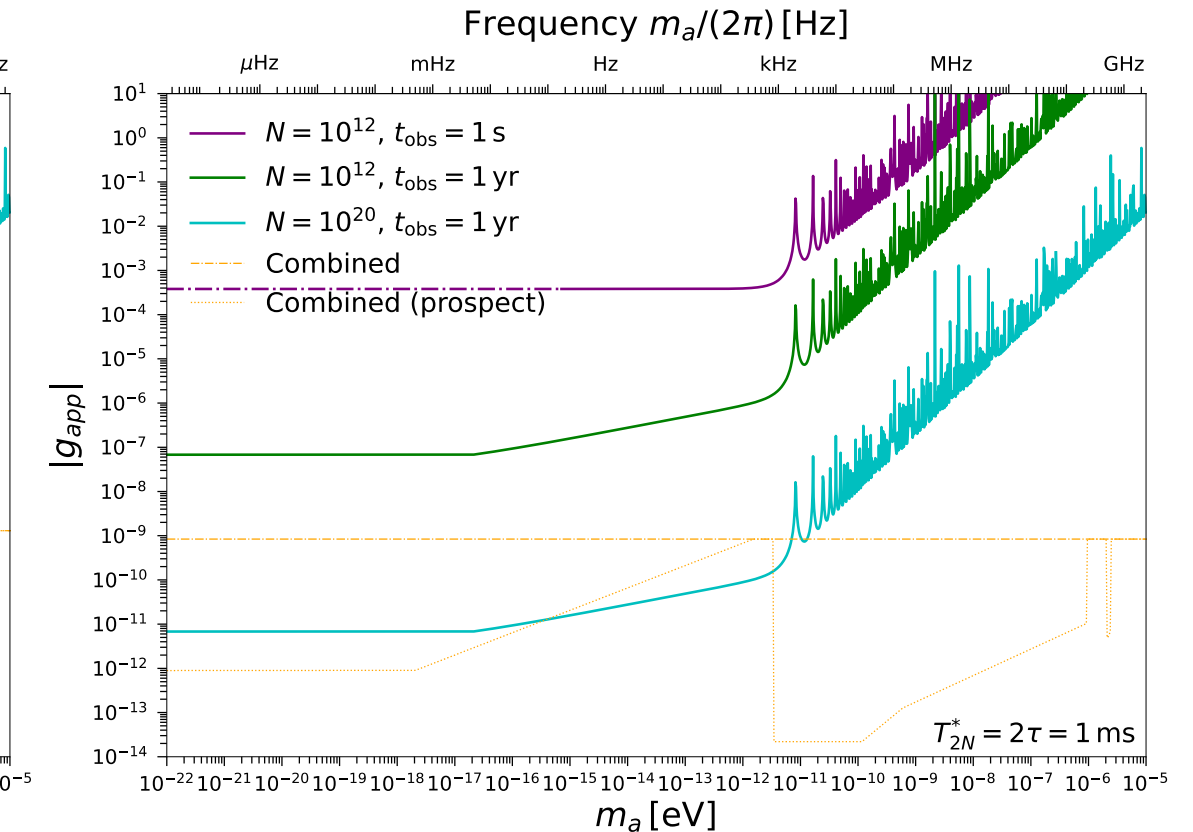
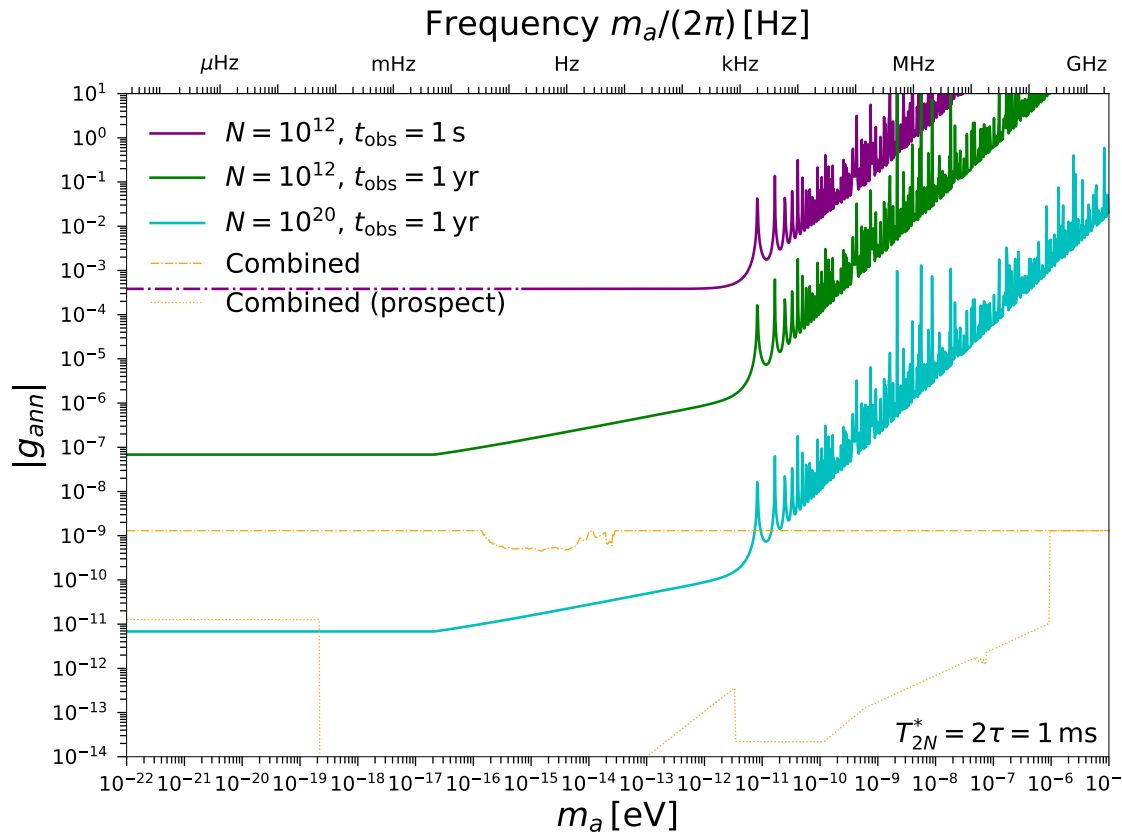
- $H_{\text{int}} = \gamma_n \vec{B}_a^{(n)} \cdot \vec{S}_n + \gamma_p \vec{B}_a^{(p)} \cdot \vec{S}_p$

$$= \gamma_{^{14}\text{N}} \vec{B}_a \cdot \vec{I} + \dots$$

$$|\vec{B}_a| \propto \frac{1}{6} \left(\frac{g_{\text{ann}}}{m_n} + \frac{g_{\text{app}}}{m_p} \right)$$



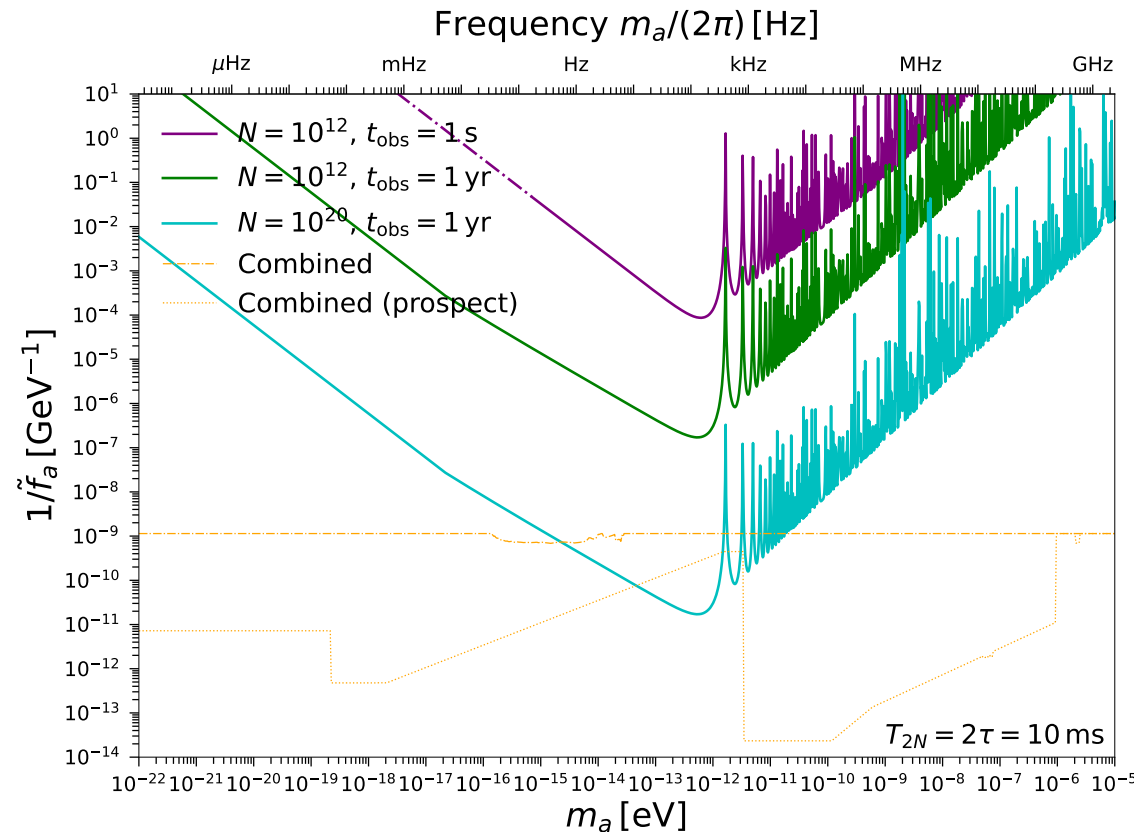
Constraints on g_{ann} and g_{app}



Hahn-echo sequence of ^{14}N spins

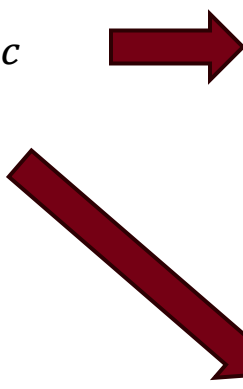
- $T_2 \sim 9\text{ms}$ is observed

Aslam, et al. '17



Single-qubit model with random noise/signal

- $H = \lambda f(t) g(t) \hat{\sigma}_z$
- λ : noise/signal amplitude
- $f(t)$: normalized random function with $\langle f(t) \rangle = 0$
 - Model of relaxation process: $\langle f(t)f(0) \rangle = e^{-|t|/\tau_c}$
 - External noise: $\langle f(t)f(0) \rangle = \int \frac{d\omega}{2\pi} e^{-i\omega t} P(\omega)$
 - Axion signal: $\langle f(t)f(0) \rangle = \cos(m_a t) \Theta(\tau_a - |t|)$
- $g(t)$: filter function
 - Ordinary magnetic field: $\gamma_N \Theta(\tau_N - t) + \gamma_e \Theta(t - \tau_N)$
 - Axion signal: $\frac{1}{3\tilde{f}_a} \Theta(\tau_N - t) + \frac{g_{aee}}{m_e} \Theta(t - \tau_N)$



Dephasing $\propto e^{-(\tau_e/T_{2e}^*)^2}$
From noises with
 $\tau_e \ll \tau_c \ll \tau_N$

Successful noise cancel
(next slide)